



US 20150079494A1

(19) **United States**

(12) **Patent Application Publication**

**Lin et al.**

(10) **Pub. No.: US 2015/0079494 A1**

(43) **Pub. Date: Mar. 19, 2015**

(54) **SOLID OXIDE FUEL CELL INTERCONNECT CELLS**

(60) Provisional application No. 61/560,177, filed on Nov. 15, 2011.

(71) Applicant: **Saint-Gobain Ceramics & Plastic, Inc.**, Worcester, MA (US)

**Publication Classification**

(72) Inventors: **Guangyong Lin**, Shrewsbury, MA (US); **Yeshwanth Narendar**, Westford, MA (US); **John D. Pietras**, Sutton, MA (US); **Qiang Zhao**, Yardley, PA (US); **Robert J. Sliwoski**, West Boylston, MA (US); **Caroline Levy**, Montpellier (FR); **Samuel S. Marlin**, Plan d'Orgon (FR); **Aravind Mohanram**, Northborough, MA (US)

(51) **Int. Cl.**  
*H01M 8/02* (2006.01)  
*H01M 8/24* (2006.01)  
*H01M 8/12* (2006.01)  
(52) **U.S. Cl.**  
CPC ..... *H01M 8/0217* (2013.01); *H01M 8/12* (2013.01); *H01M 8/2465* (2013.01); *H01M 2008/1293* (2013.01)  
USPC ..... **429/465**; 429/510

(21) Appl. No.: **14/551,343**

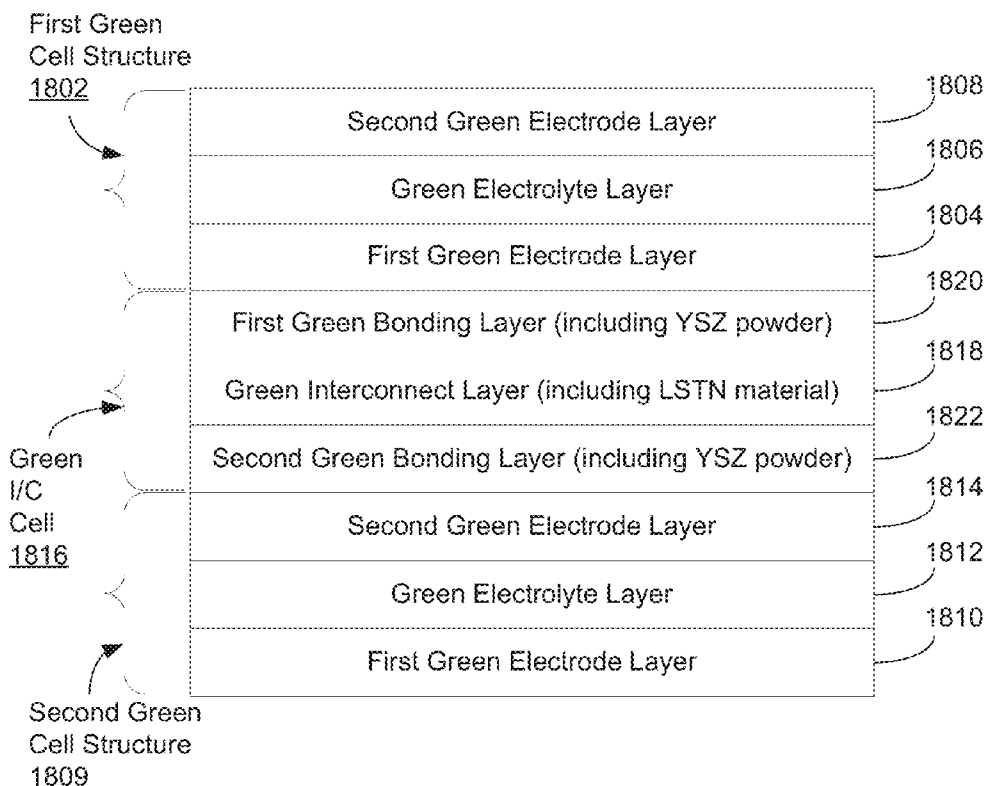
**ABSTRACT**

(22) Filed: **Nov. 24, 2014**

A bonding layer, disposed between an interconnect layer and an electrode layer of a solid oxide fuel cell article, may be formed from a yttria stabilized zirconia (YSZ) powder having a monomodal particle size distribution (PSD) with a  $d_{50}$  that is greater than about 1  $\mu\text{m}$  and a  $d_{90}$  that is greater than about 2  $\mu\text{m}$ .

**Related U.S. Application Data**

(63) Continuation of application No. 13/676,838, filed on Nov. 14, 2012, now Pat. No. 8,921,007.



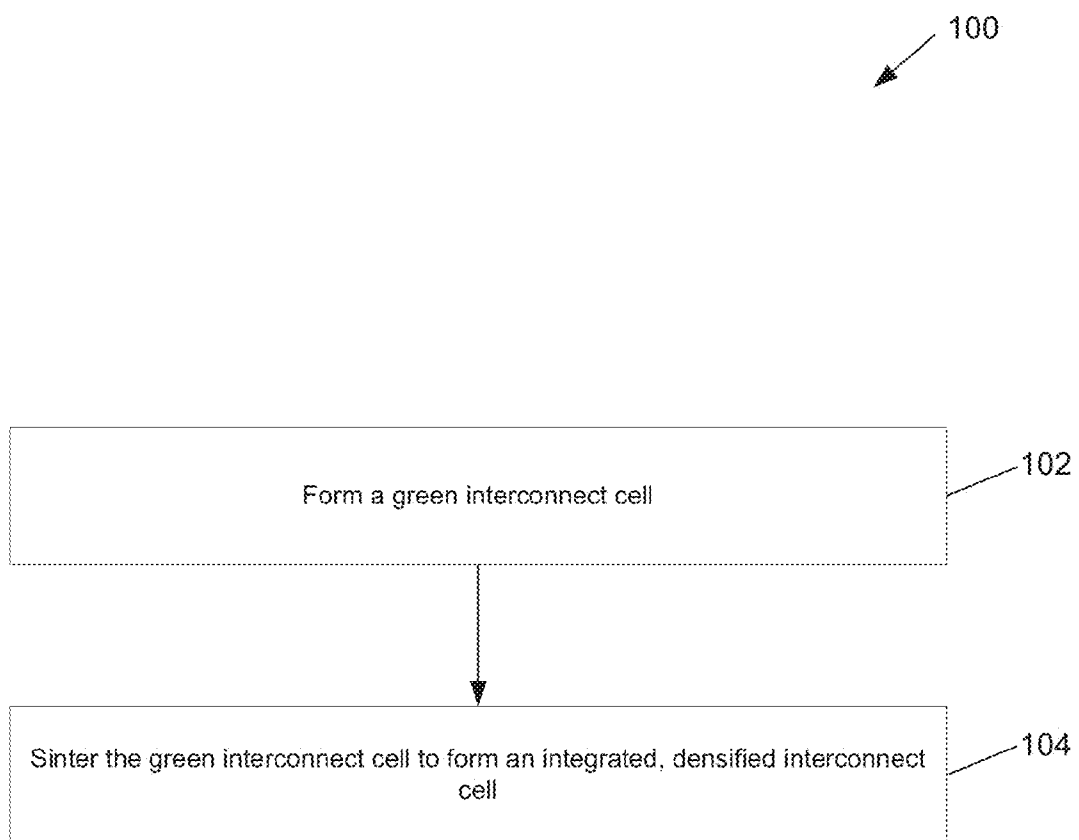


**FIG. 1**

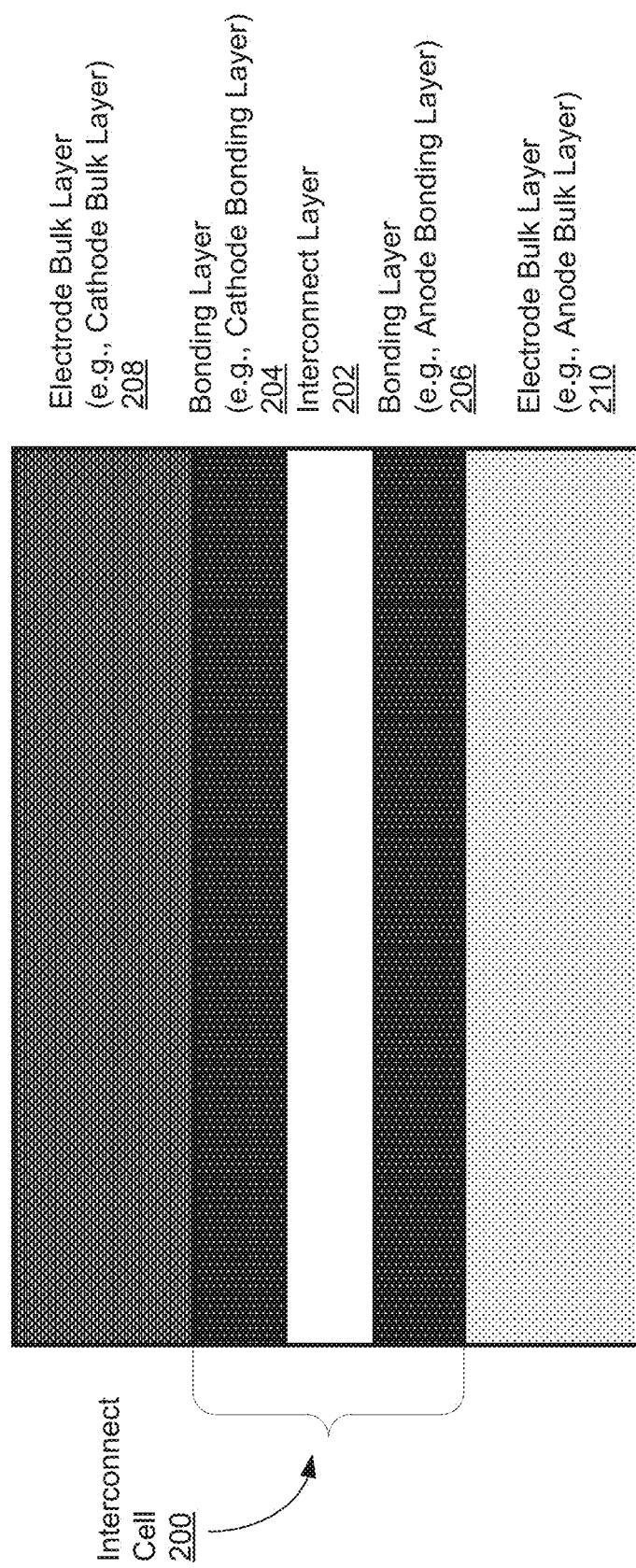
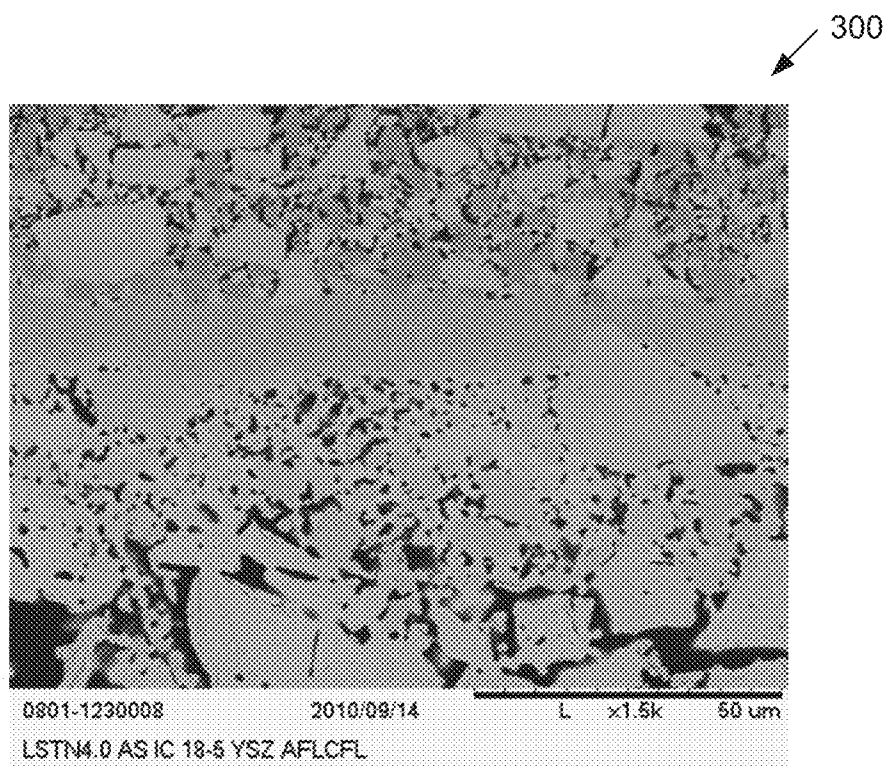
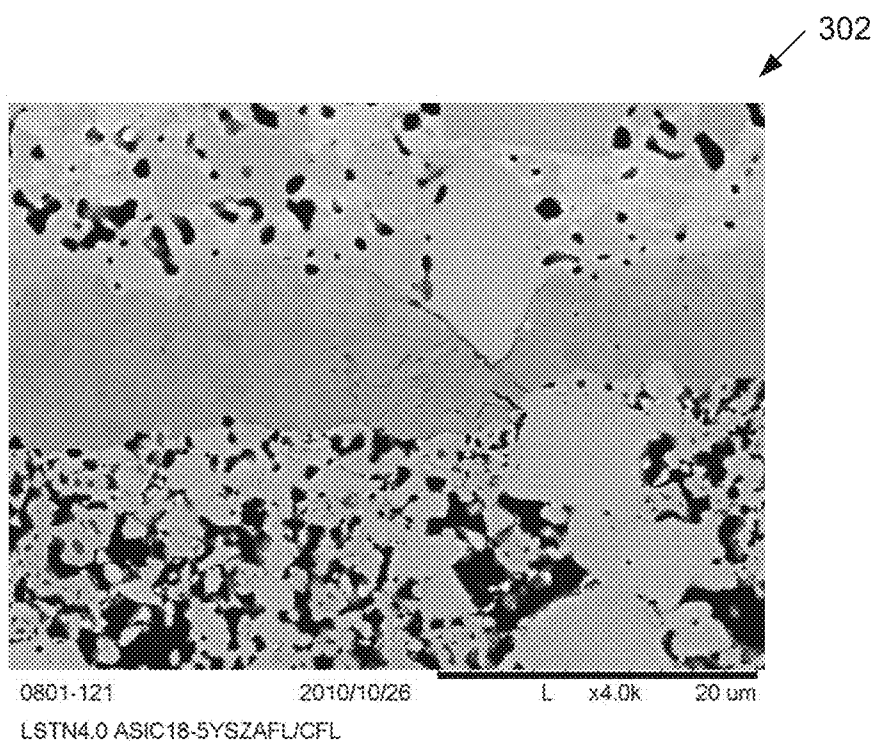


FIG. 2



**FIG. 3A**



**FIG. 3B**

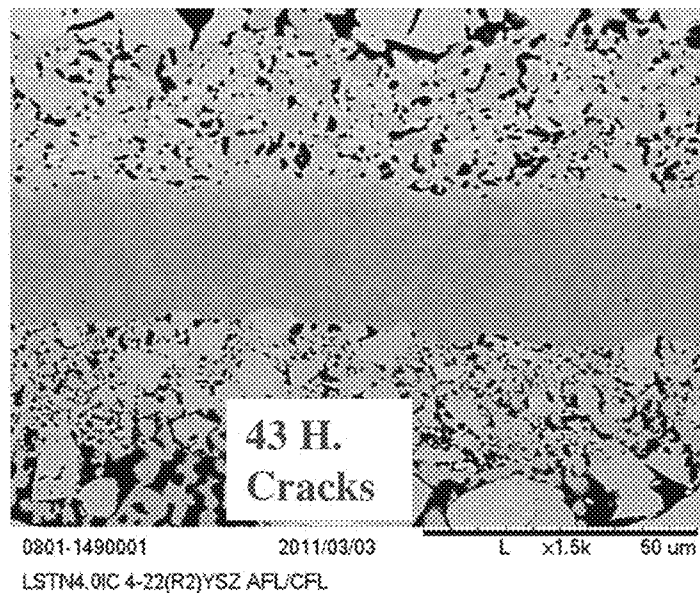


*FIG. 4*

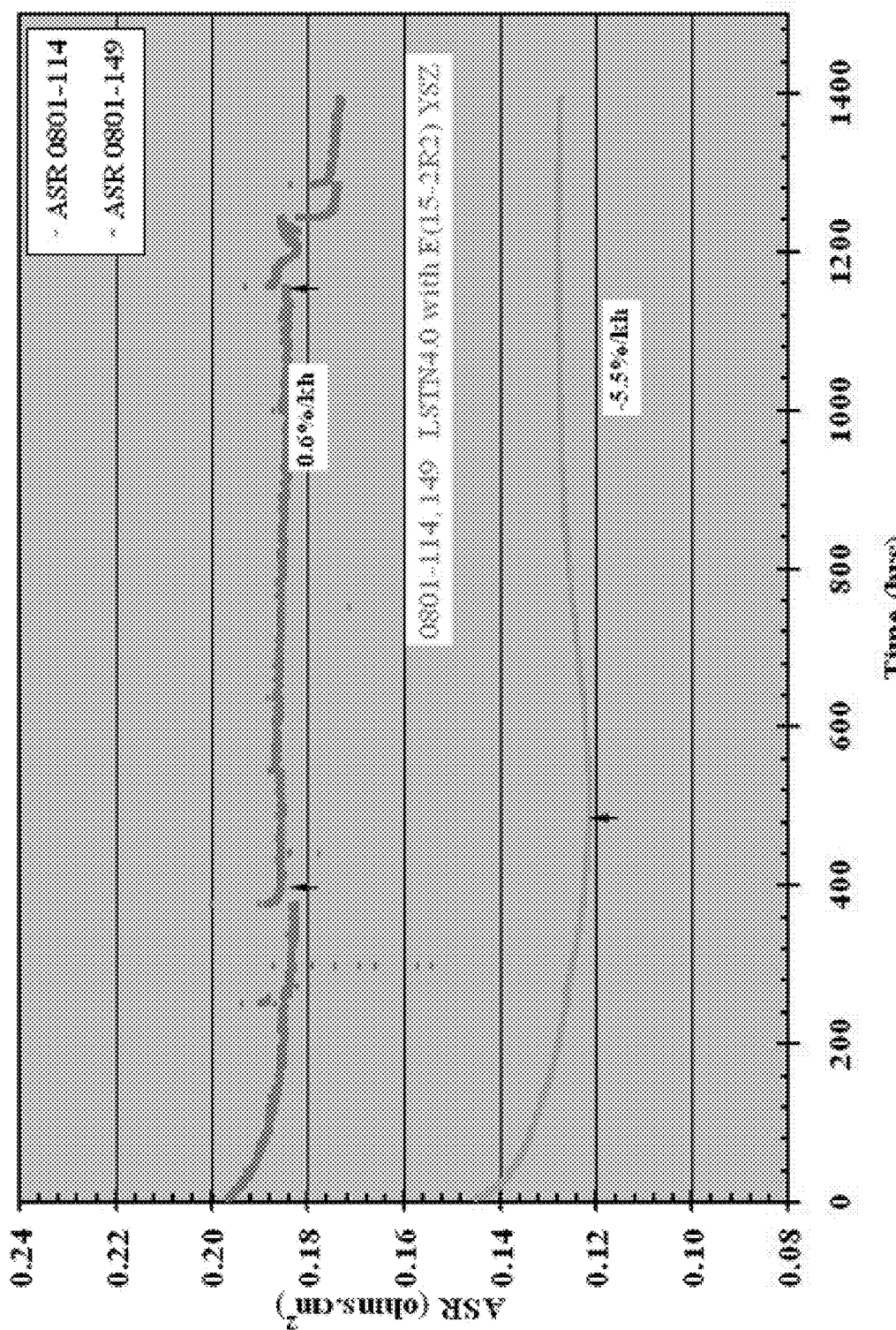
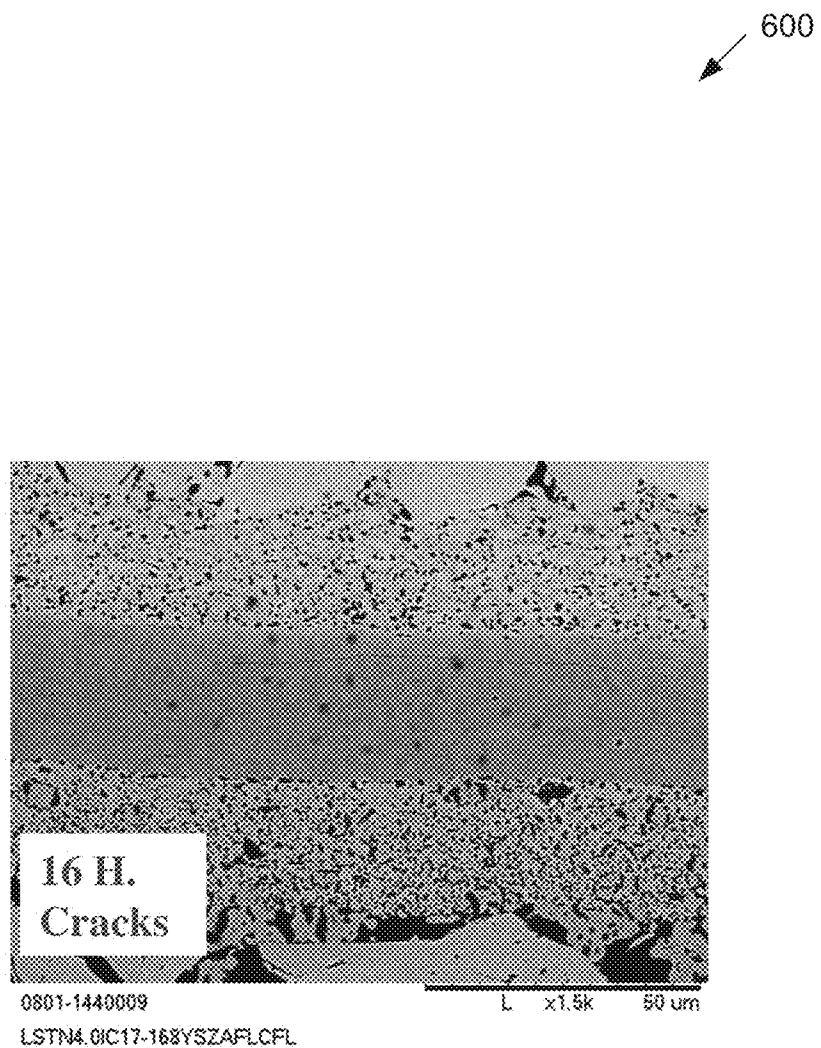


FIG. 5



*FIG. 6*

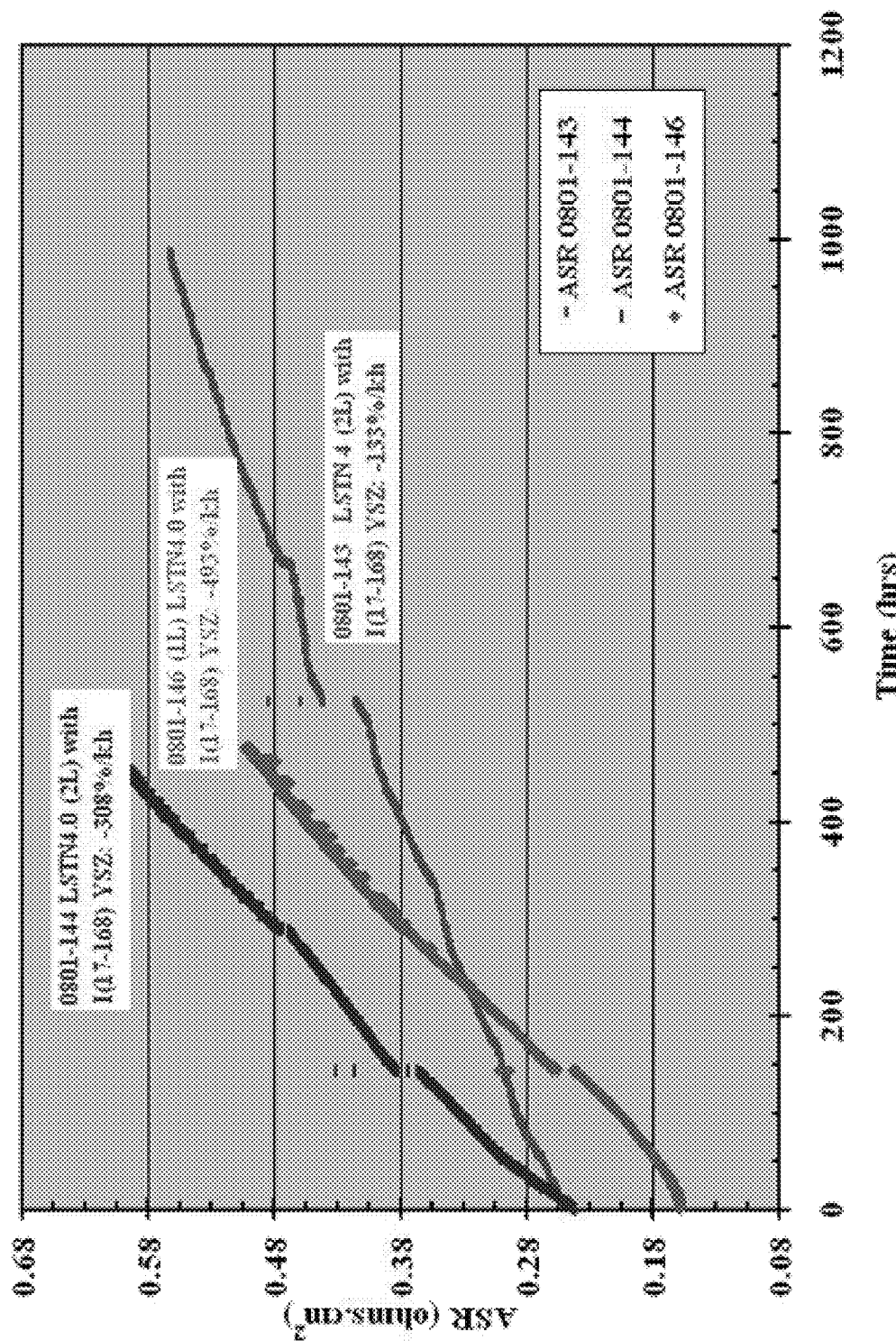
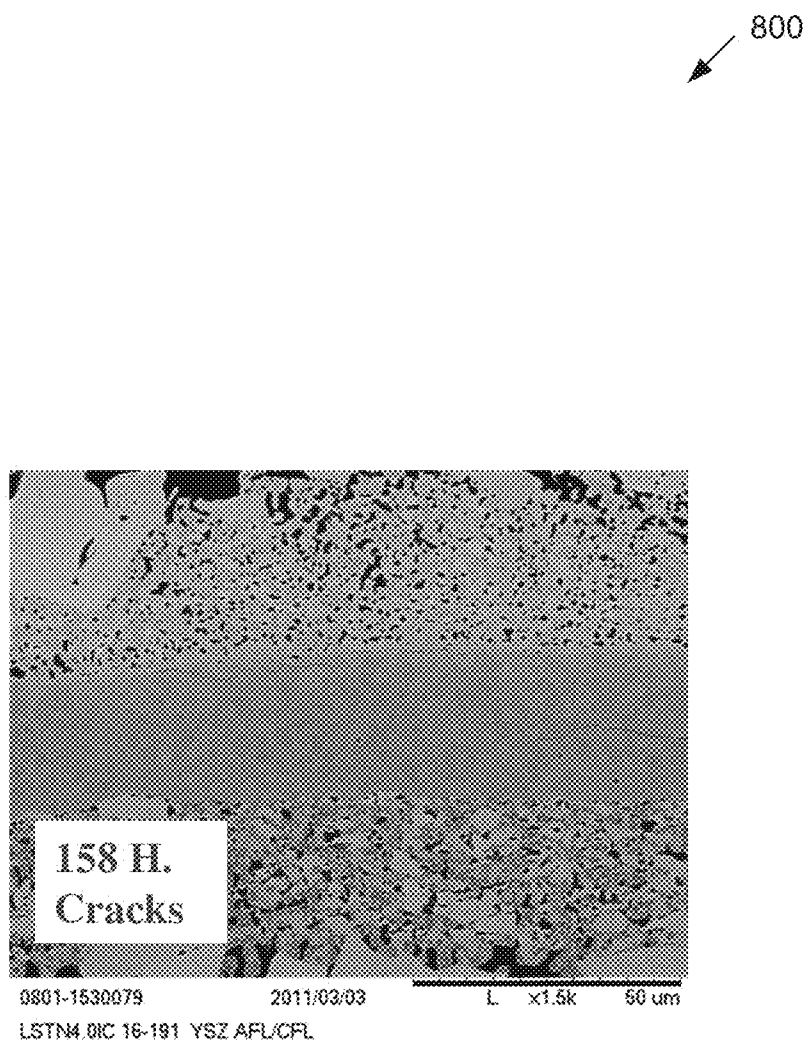
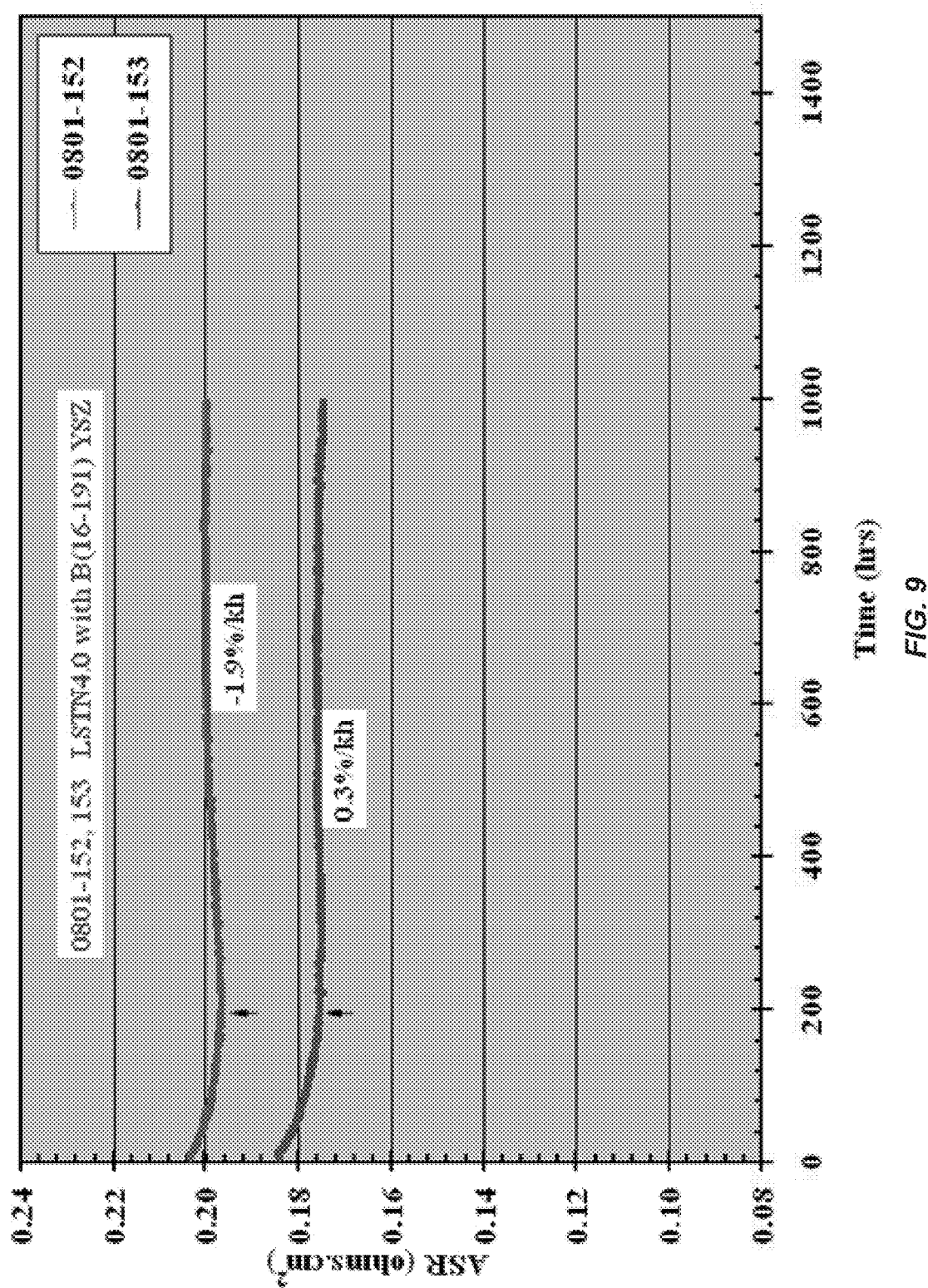
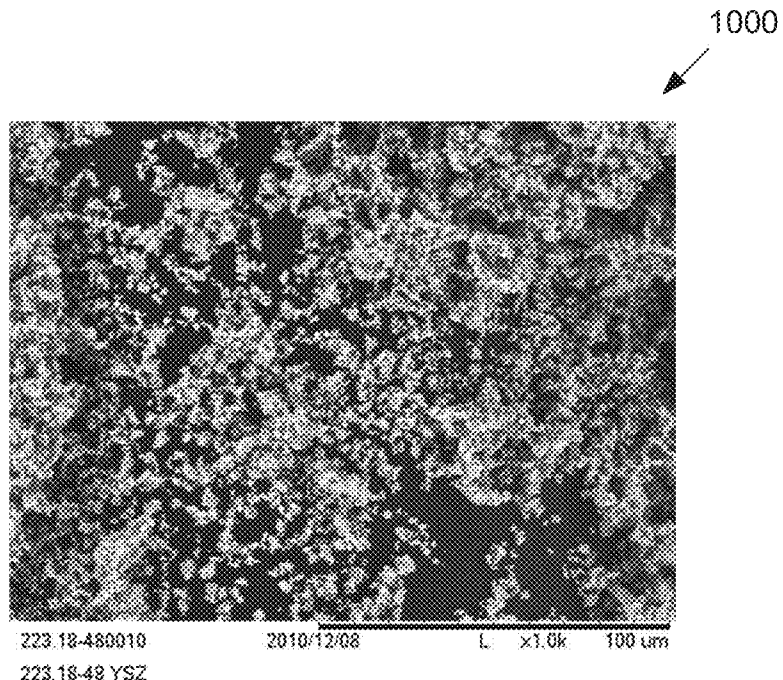


FIG. 7



*FIG. 8*





*FIG. 10*

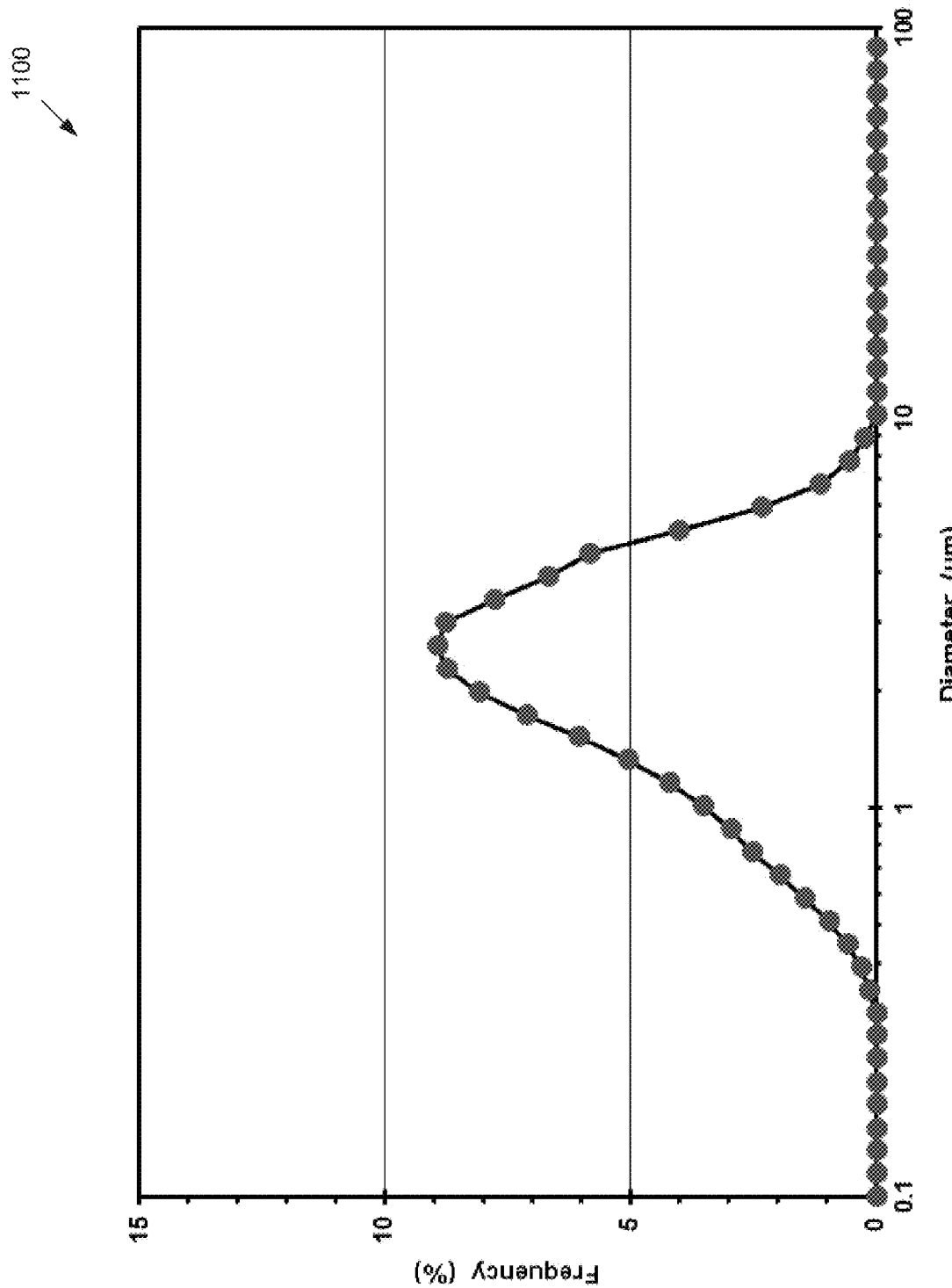


FIG. 11

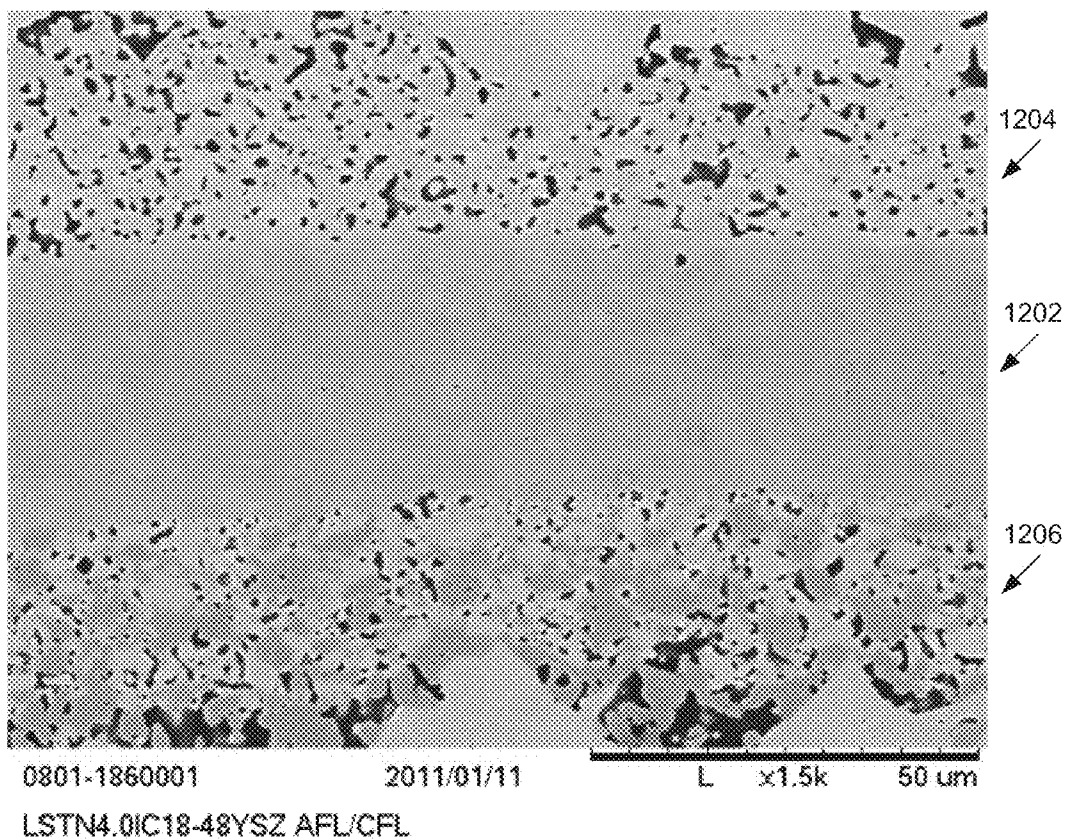


FIG. 12

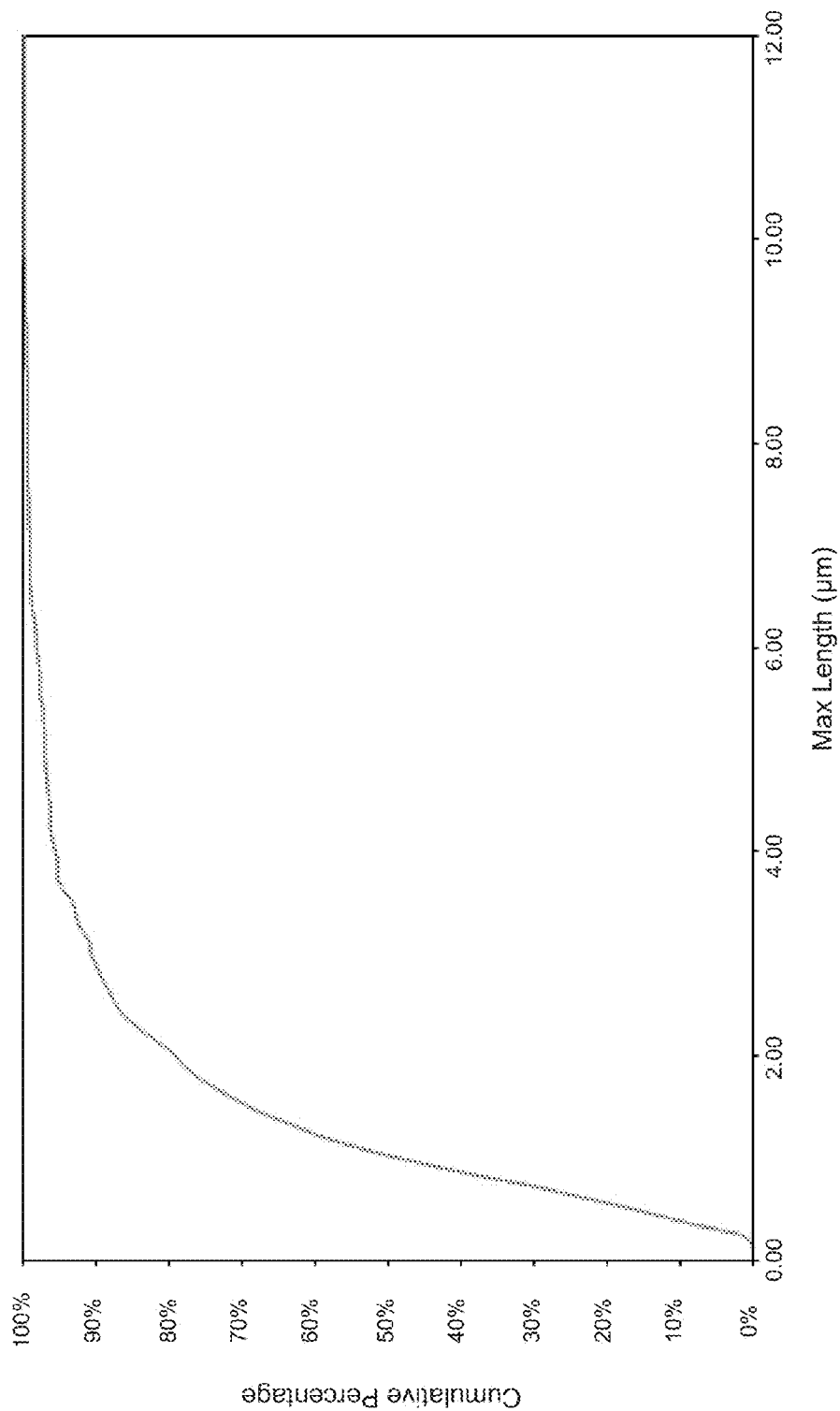


FIG. 13

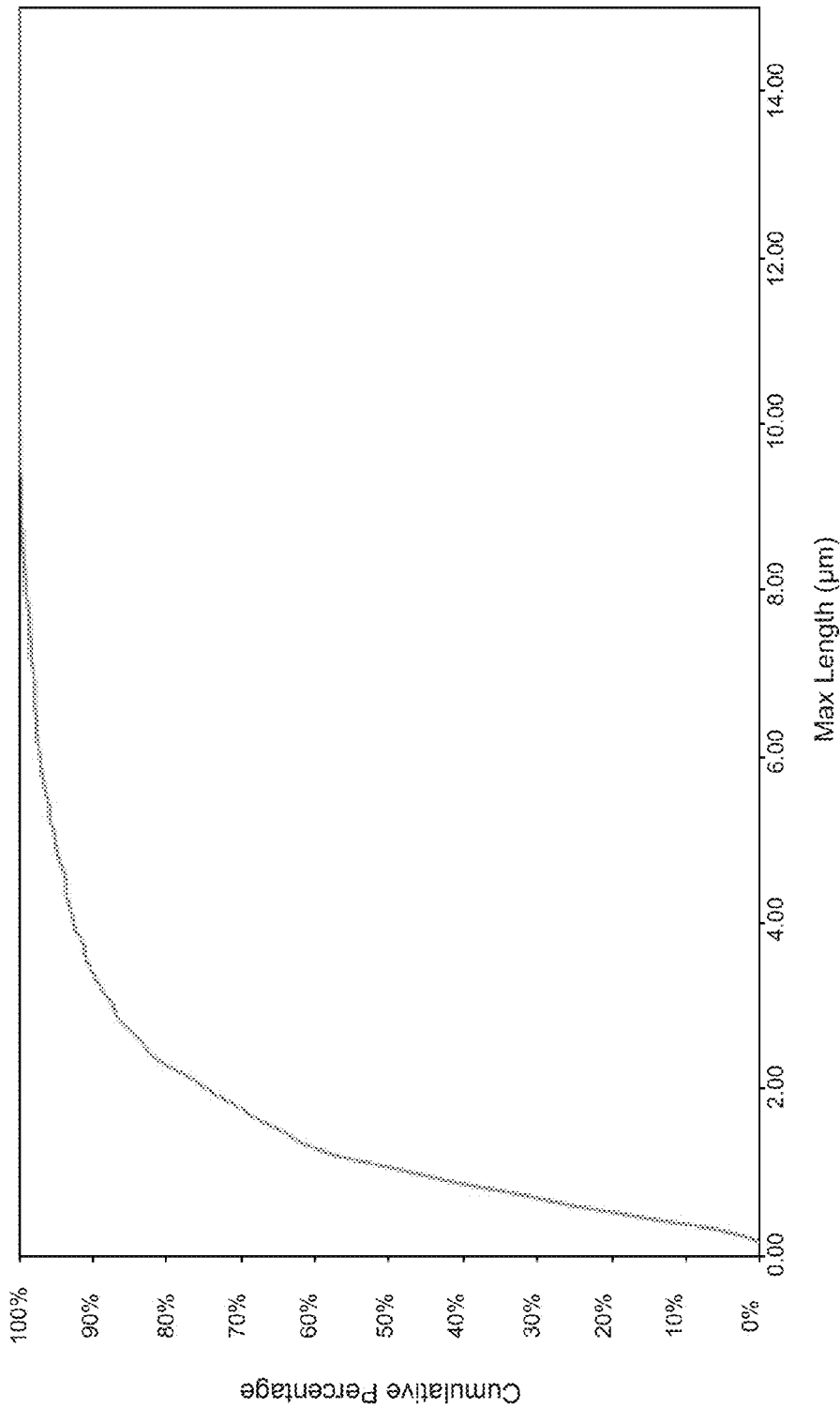


FIG. 14

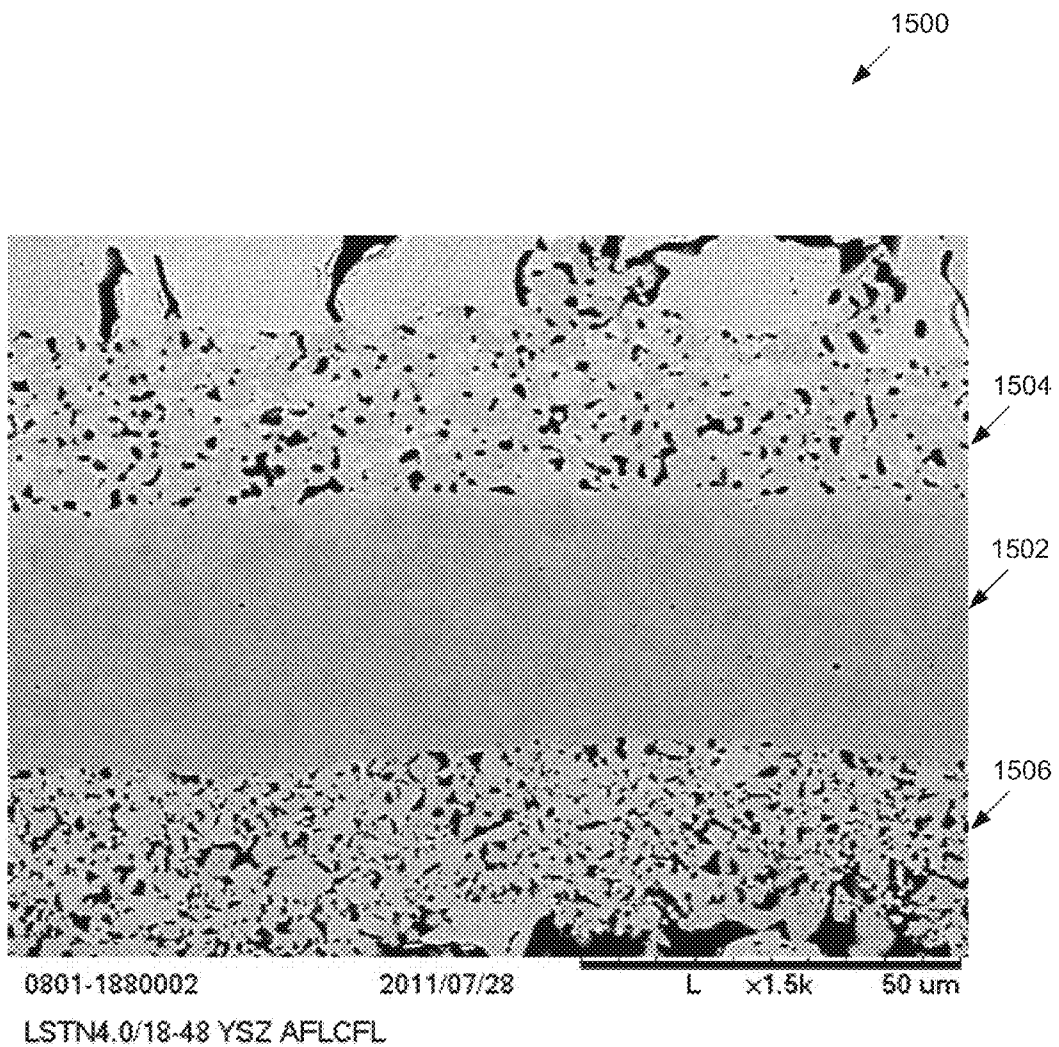


FIG. 15

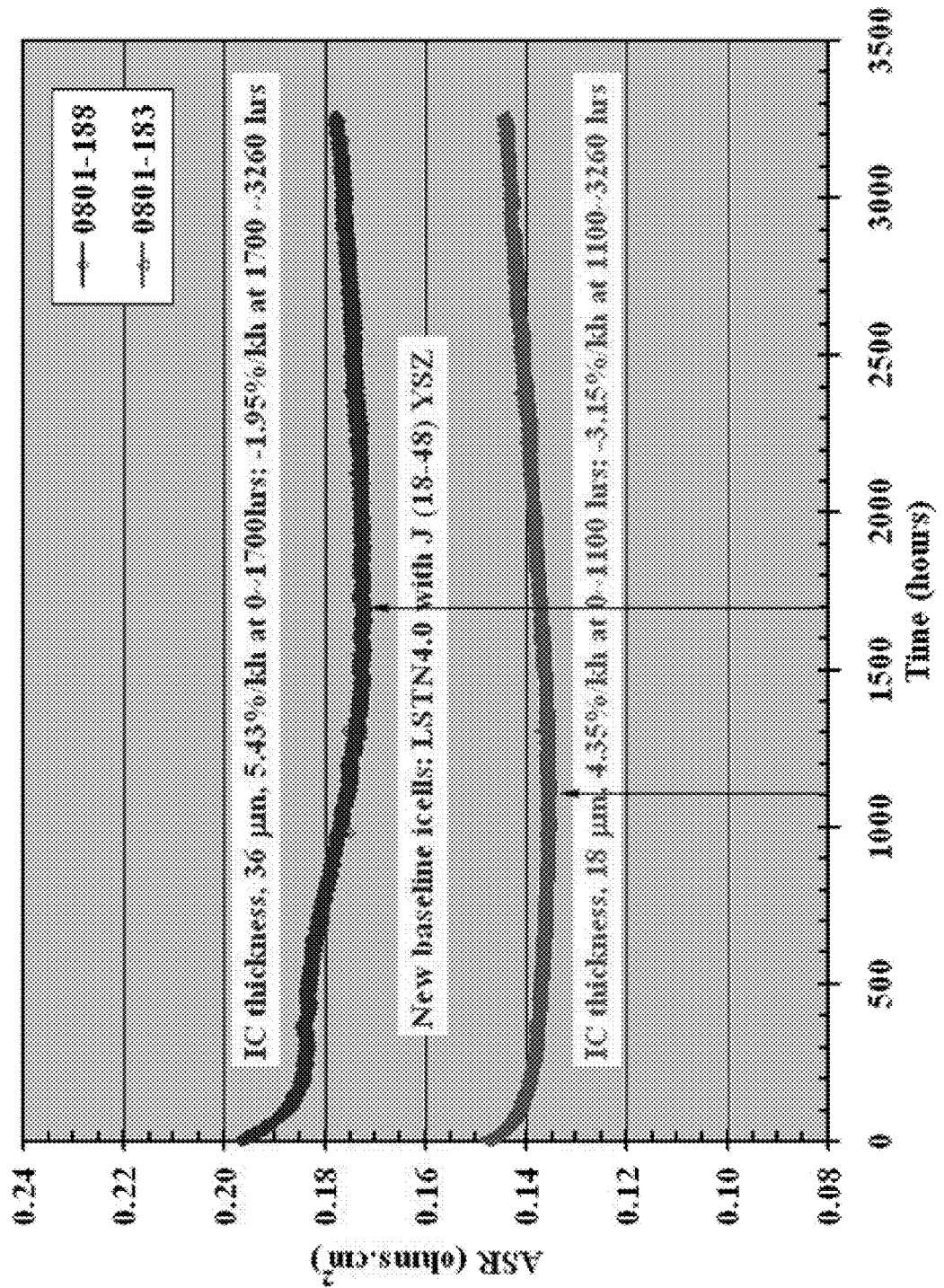


FIG. 16

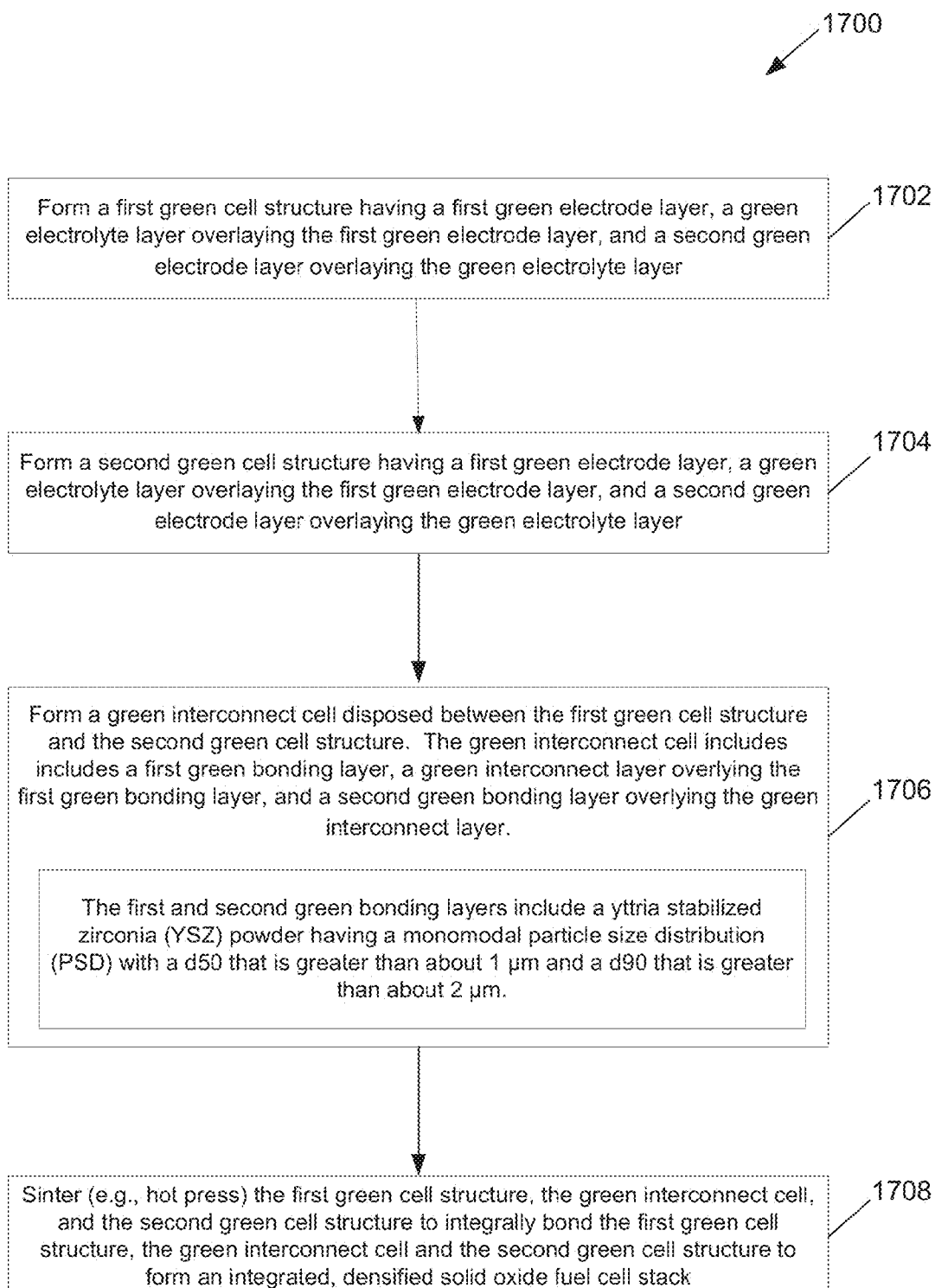


FIG. 17

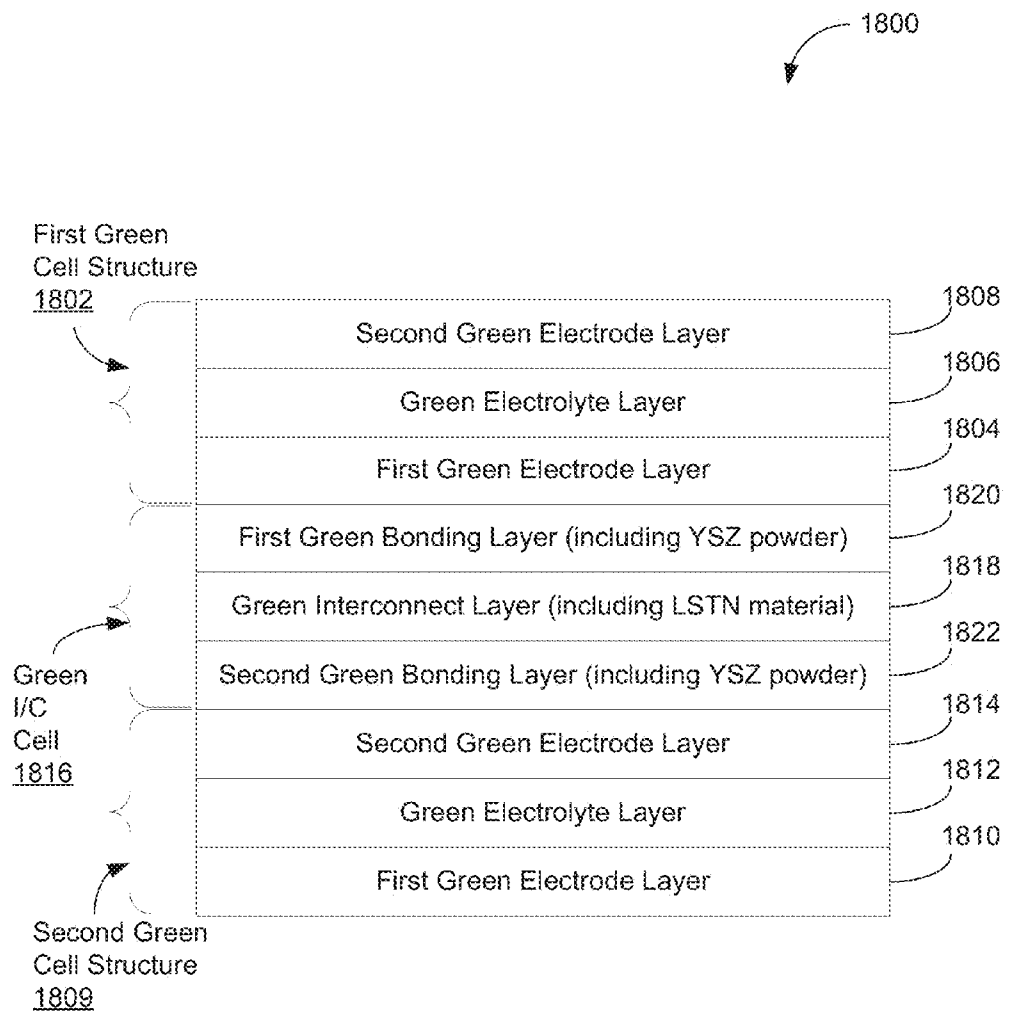


FIG. 18

## SOLID OXIDE FUEL CELL INTERCONNECT CELLS

### CROSS-REFERENCE TO RELATED APPLICATIONS

[0001] This application is a continuation application of and claims priority under 35 U.S.C. §120 to U.S. patent application Ser. No. 13/676,838, filed Nov. 14, 2012, entitled "SOLID OXIDE FUEL CELL INTERCONNECT CELLS" naming inventors Guangyong Lin et al., which claims priority to U.S. Patent Application No. 61/560,177, entitled "Solid Oxide Fuel Cell Interconnect Cells," naming inventors Guangyong Lin et al., filed Nov. 15, 2011, both of which are assigned to the current assignee hereof and incorporated by reference herein in their entireties.

### FIELD OF THE DISCLOSURE

[0002] The present disclosure is related to solid oxide fuel cells (SOFCs).

### DESCRIPTION OF THE RELATED ART

[0003] A fuel cell is a device that generates electricity by a chemical reaction. Among various fuel cells, solid oxide fuel cells (SOFCs) use a hard, ceramic compound metal (e.g., calcium or zirconium) oxide as an electrolyte. Typically, in solid oxide fuel cells, an oxygen gas, such as O<sub>2</sub>, is reduced to oxygen ions (O<sup>2-</sup>) at the cathode, and a fuel gas, such as H<sub>2</sub> gas, is oxidized with the oxygen ions to form water at the anode.

[0004] In some instances, fuel cell assemblies have been designed as stacks, which include a cathode, anode, and solid electrolyte between the cathode and the anode. Each stack can be considered a subassembly, which can be combined with other stacks to form a full SOFC article. In assembling the SOFC article, electrical interconnects can be disposed between the cathode of one stack and the anode of another stack.

[0005] However, stacks of individual fuel cells can be susceptible to damage caused by fluctuation in temperature during their formation or use. Specifically, materials employed to form the various components, including ceramics of differing compositions, exhibit distinct material, chemical, and electrical properties that can result in breakdown and failure of the SOFC article. In particular, fuel cells have a limited tolerance for changes in temperature. Problems associated with mechanical stress caused by changes in temperature are exacerbated when individual fuel cells are stacked. Limited thermal shock resistance of fuel cells, particularly of fuel cells assembled in stacks, limits the yield of production and poses a heightened risk of failure during operation. What is needed is an improved bonding layer for use with stacked fuel cells.

### SUMMARY

[0006] According to one embodiment, a bonding layer of a solid oxide fuel cell article is disclosed. The bonding layer is disposed between an interconnect layer and an electrode layer of the solid oxide fuel cell article. The bonding layer may be formed from a yttria stabilized zirconia (YSZ) powder having a monomodal particle size distribution (PSD) with a d<sub>50</sub> that is greater than about 1 μm and a d<sub>90</sub> that is greater than about 2 μm.

[0007] According to another embodiment, an interconnect cell of a solid oxide fuel cell stack is disclosed. The intercon-

nect cell includes an interconnect layer, a cathode bonding layer, and an anode bonding layer. The cathode bonding layer is disposed between the interconnect layer and a cathode layer of the solid oxide fuel cell stack, and the anode bonding layer is disposed between the interconnect layer and an anode layer of the solid oxide fuel cell stack. The cathode bonding layer is formed from a YSZ powder having a monomodal PSD with a d<sub>50</sub> that is greater than about 1 μm and a d<sub>90</sub> that is greater than about 2 μm. Further, the anode bonding layer is formed from a YSZ powder having a monomodal PSD with a d<sub>50</sub> that is greater than about 1 μm and a d<sub>90</sub> that is greater than about 2 μm.

[0008] According to another embodiment, an interconnect cell of a solid oxide fuel cell stack is disclosed. The interconnect cell includes an interconnect layer, a cathode bonding layer, and an anode bonding layer. The cathode bonding layer is disposed between the interconnect layer and a cathode layer of the solid oxide fuel cell stack, and the anode bonding layer is disposed between the interconnect layer and an anode layer of the solid oxide fuel cell stack. The cathode bonding layer and the anode bonding layer include yttria stabilized zirconia. The interconnect cell reaches a Steady State Area Specific Resistance (ASR) (ohms·cm<sup>2</sup>) within a time period of not less than about 600 hours of operation.

[0009] According to another embodiment, a solid oxide fuel cell stack is disclosed that includes a first electrode layer, a first electrolyte layer overlying the first electrode layer, a second electrode layer overlying the first electrolyte layer, and an interconnect cell disposed between the second electrode layer and a third electrode layer. A second electrolyte layer overlies the third electrode layer, and a fourth electrode layer overlies the second electrolyte layer. The interconnect cell includes an interconnect layer, a first bonding layer, and a second bonding layer. The first bonding layer includes YSZ and is disposed between the interconnect layer and the second electrode layer. The first bonding layer is formed from a YSZ powder having a monomodal PSD with a d<sub>50</sub> that is greater than about 1 μm and a d<sub>90</sub> that is greater than about 2 μm. The second bonding layer includes YSZ and is disposed between the interconnect layer and the third electrode layer. The second bonding layer is formed from a YSZ powder having a monomodal PSD with a d<sub>50</sub> that is greater than about 1 μm and a d<sub>90</sub> that is greater than about 2 μm.

[0010] According to yet another embodiment, a solid oxide fuel cell stack is disclosed that includes a first electrode layer, a first electrolyte layer overlying the first electrode layer, a second electrode layer overlying the first electrolyte layer, and an interconnect cell disposed between the second electrode layer and a third electrode layer. A second electrolyte layer overlies the third electrode layer, and a fourth electrode layer overlies the second electrolyte layer. The interconnect cell includes an interconnect layer, a first bonding layer, and a second bonding layer. The first bonding layer includes YSZ and is disposed between the interconnect layer and the second electrode layer. The second bonding layer includes YSZ and is disposed between the interconnect layer and the third electrode layer. The interconnect cell reaches a Steady State Area Specific Resistance (ASR) (ohms·cm<sup>2</sup>) within a time period of not less than about 600 hours of operation.

[0011] According to yet another embodiment, a method of forming an interconnect cell of a solid oxide fuel cell stack includes forming a green interconnect cell. The green interconnect cell includes a first green bonding layer that includes a YSZ powder having a monomodal PSD with a d<sub>50</sub> that is

greater than about 1  $\mu\text{m}$  and a  $d_{90}$  that is greater than about 2  $\mu\text{m}$ . The green interconnect cell further includes a green interconnect layer overlying the first green bonding layer and a second green bonding layer overlying the green interconnect layer. The second green bonding layer includes a YSZ powder having a monomodal PSD with a  $d_{50}$  that is greater than about 1  $\mu\text{m}$  and a  $d_{90}$  that is greater than about 2  $\mu\text{m}$ . The method further includes sintering the first green bonding layer, the green interconnect layer, and the second green bonding layer to integrally bond the first green bonding layer, the green interconnect layer, and the second green bonding layer to form an integrated, densified interconnect cell.

[0012] According to another embodiment, a method of forming an integrated SOFC stack is disclosed. The method includes forming a first green cell structure having a first green electrode layer, a green electrolyte layer overlying the first green electrode layer, and a second green electrode layer overlying the green electrolyte layer. The method includes forming a second green cell structure having a first green electrode layer, a green electrolyte layer overlying the first green electrode layer, and a second green electrode layer overlying the green electrolyte layer. The method further includes forming a green interconnect cell disposed between the first green cell structure and the second green cell structure. The green interconnect cell includes a green interconnect layer, a first green bonding layer, and a second green bonding layer. The first green bonding layer is disposed between the interconnect layer and the first green cell structure, and the second green bonding layer is disposed between the interconnect layer and the second green cell structure. The first green bonding layer includes a YSZ powder having a monomodal PSD with a  $d_{50}$  that is greater than 1  $\mu\text{m}$  and a  $d_{90}$  that is greater than 2  $\mu\text{m}$ . The second green bonding layer includes a YSZ powder having a monomodal PSD with a  $d_{50}$  that is greater than 1  $\mu\text{m}$  and a  $d_{90}$  that is greater than 2  $\mu\text{m}$ . The method further includes sintering the first green cell structure, the green interconnect cell, and the second green cell structure to integrally bond the first green cell structure, the green interconnect cell and the second green cell structure to form an integrated SOFC stack.

#### BRIEF DESCRIPTION OF THE DRAWINGS

[0013] The present disclosure may be better understood, and its numerous features and advantages made apparent to those skilled in the art by referencing the accompanying drawings.

[0014] FIG. 1 illustrates a method of forming an interconnect cell of a solid oxide fuel cell stack according to an embodiment.

[0015] FIG. 2 is an illustration of an interconnect cell disposed between two electrode bulk layers of the SOFC stack in accordance with an embodiment.

[0016] FIG. 3A is a cross-sectional SEM image of an interconnect cell that includes bonding layers formed from a first bimodal YSZ powder, prior to electrochemical testing.

[0017] FIG. 3B is a cross-sectional SEM image of the interconnect cell of FIG. 3A after electrochemical testing, illustrating puncturing effects and resulting interconnect cracking.

[0018] FIG. 4 is a cross-sectional SEM image of an interconnect cell formed from a second bimodal YSZ powder, showing interconnect cracking after long term testing.

[0019] FIG. 5 illustrates the area specific resistance (ASR) ( $\text{ohms}\cdot\text{cm}^2$ ) over the course of the long term testing of the interconnect cell formed from the second bimodal YSZ powder.

[0020] FIG. 6 is a cross-sectional SEM image of an interconnect cell formed from a first monomodal YSZ powder, showing interconnect cracking after long term testing.

[0021] FIG. 7 illustrates the area specific resistance (ASR) ( $\text{ohms}\cdot\text{cm}^2$ ) over the course of the long term testing of the interconnect cell formed from the first monomodal YSZ powder.

[0022] FIG. 8 is a cross-sectional SEM image of an interconnect cell formed from a second monomodal YSZ powder, showing interconnect cracking after long term testing.

[0023] FIG. 9 illustrates the area specific resistance (ASR) ( $\text{ohms}\cdot\text{cm}^2$ ) over the course of the long term testing of the interconnect cell formed from the second monomodal YSZ powder.

[0024] FIG. 10 is an SEM image of an exemplary YSZ powder that may be utilized for formation of a bonding layer according to an embodiment.

[0025] FIG. 11 illustrates the particle size distribution of the exemplary YSZ powder of FIG. 10.

[0026] FIG. 12 is a cross-sectional SEM image of an interconnect cell according to an embodiment. The bonding layers of the interconnect cell illustrated in FIG. 12 were formed from the exemplary YSZ powder of FIG. 10.

[0027] FIG. 13 illustrates the pore size distribution of the cathode bonding layer of the interconnect cell illustrated in FIG. 12.

[0028] FIG. 14 illustrates the pore size distribution of the anode bonding layer of the interconnect cell illustrated in FIG. 12.

[0029] FIG. 15 is a cross-sectional SEM image of an interconnect cell according to an embodiment after long term testing, showing no interconnect cracking. The bonding layers of the interconnect cell illustrated in FIG. 15 were formed from the exemplary YSZ powder of FIG. 10.

[0030] FIG. 16 illustrates the results of long term testing of the area specific resistance (ASR) ( $\text{ohms}\cdot\text{cm}^2$ ) of exemplary interconnect cells according to embodiments described herein.

[0031] FIG. 17 illustrates a method of forming an integrated solid oxide fuel cell stack according to an embodiment.

[0032] FIG. 18 illustrates a particular embodiment of a green SOFC cell stack according to an embodiment.

[0033] The use of the same reference symbols in different drawings indicates similar or identical items.

#### DESCRIPTION

[0034] The present disclosure is related to solid oxide fuel cell (SOFC) articles including SOFC stacks and methods of forming the SOFC stacks. A material that includes yttria stabilized zirconia (YSZ) with a particular particle size distribution (PSD) may be used in bonding layers that are disposed between an interconnect layer and electrodes of different SOFC cells of an SOFC stack. Interconnect cells that include bonding layers formed from such YSZ powders may exhibit improved long term performance.

[0035] Referring to FIG. 1, a particular embodiment of a method of forming an interconnect cell of a solid oxide fuel cell stack is illustrated and generally designated **100**. The method **100** includes forming a green interconnect cell, at **102**. In a particular embodiment, the green interconnect cell

can include a green bonding layer that includes a YSZ powder having a monomodal PSD with a  $d_{50}$  that can be greater than 0.7  $\mu\text{m}$  and a  $d_{90}$  that can be 1.5  $\mu\text{m}$  or greater; more preferably the YSZ powder can have with a  $d_{50}$  that can be greater than 1  $\mu\text{m}$  and a  $d_{90}$  that can be greater than 2  $\mu\text{m}$ . In some embodiments the YSZ powder can have with a  $d_{50}$  that can be greater than 2  $\mu\text{m}$  and a  $d_{90}$  that can be greater than 4  $\mu\text{m}$ . In a particular embodiment, the green interconnect cell further includes a green interconnect layer overlying the green bonding layer and a second green bonding layer overlying the green interconnect layer. The second green bonding layer may include a YSZ powder having a monomodal PSD with a  $d_{50}$  that can be greater than 0.7  $\mu\text{m}$  and a  $d_{90}$  that can be 1.5  $\mu\text{m}$  or greater, more preferably a  $d_{50}$  greater than 1  $\mu\text{m}$  and a  $d_{90}$  greater than 2  $\mu\text{m}$ . In some embodiments the YSZ powder can have with a  $d_{50}$  that can be greater than 2  $\mu\text{m}$  and a  $d_{90}$  that can be greater than 4  $\mu\text{m}$ . Coarse particles in the bonding layers may have a puncturing effect. As such, in a particular embodiment, not less than 99 vol % of particles of the green YSZ powder have a particle size diameter that is less than 10  $\mu\text{m}$ .

[0036] The method 100 further includes sintering the green interconnect cell to form an integrated, densified interconnect cell, at 104. In a particular embodiment, sintering the green interconnect cell includes sintering (e.g., free sintering, hot pressing) a first green bonding layer, the green interconnect layer, and a second green bonding layer to integrally bond the first green bonding layer, the green interconnect layer, and the second green bonding layer.

[0037] Applicants have discovered that an SOFC unit cell including an interconnect cell that includes a bonding layer formed according to embodiments herein can have improved electrochemical performance. For example, cracking in the interconnect cell may be reduced. As another example, the interconnect cell may exhibit improved performance with respect to degradation of area specific resistance (ASR) during operation.

[0038] One function of an interconnect layer in an SOFC stack is as a connector to provide an electron conductor so that the electron can be transferred from one cell to another. Another function of the interconnect layer is as a gas separator to ensure that the fuel gas such as  $\text{H}_2$  or  $\text{CH}_4$  in the anode side would not mix with the oxidant such as air in the cathode directly. Any cracks in the interconnect layer may cause the reduction of the electron conduction area and may allow gas cross leakage, reducing its functions as the electron conductor and the gas separator. Therefore, any cracks in the interconnects should be avoided.

[0039] The interconnect layer provides an electron conductor and a gas separator so that the SOFC stack performance such as the power density is inversely proportional to (partially dependent on) the resistance of the interconnect layer, in the term of area specific resistance (ASR). A higher ASR of the interconnect cell may cause a lower power density of the SOFC stack. ASR degradation of the interconnect cell over time may result in reducing SOFC stack performance such as the power density degradation. Therefore, an interconnect cell with a low ASR and a low ASR degradation may allow for improving SOFC stack performance. Electrochemical ("E-chem") testing may be used to determine whether the ASR of the interconnect cell is decreasing and/or stable over time (i.e., whether there is ASR degradation).

[0040] As used herein, the term "Steady State" ASR refers to a region on a long term ASR testing curve where the ASR is lowest. That is, an ASR testing curve with ASR ( $\text{ohms}\cdot\text{cm}^2$ )

plotted on the Y axis and time (hours) plotted on the X axis, and the Steady State ASR is the ASR value in the region of the curve that has a slope of approximately zero. Said another way, the Steady State ASR is the ASR value that is measured at the approximate time when the ASR value begins to increase along the Y axis (i.e., when ASR "degradation" begins). In a particular embodiment, an interconnect cell may reach a Steady State ASR within a time period of not less than about 600 hours of operation.

[0041] In a particular embodiment, the ASR of an interconnect cell may reach the Steady State ASR within a time period of not less than about 600 hours, such as not less than about 700 hours, not less than about 800 hours, not less than about 900 hours, not less than about 1000 hours, not less than about 1100 hours, not less than about 1200 hours, not less than about 1300 hours, not less than about 1400 hours, not less than about 1500 hours, or even not less than about 1600 hours.

[0042] The layers described according to the embodiments herein can be formed through techniques including, but not limited to, casting, deposition, printing, extruding, lamination, die-pressing, gel casting, spray coating, screen printing, roll compaction, injection molding, and a combination thereof. In one particular instance, each of the layers can be formed via screen printing. In another embodiment, each of the layers can be formed via a tape casting process.

[0043] FIG. 2 includes an illustration of an interconnect cell 200 disposed between two electrodes of an SOFC stack in accordance with an embodiment. In a particular embodiment, the interconnect cell 200 of FIG. 2 may be formed via the method 100 of FIG. 1.

[0044] The interconnect cell 200 of FIG. 2 includes an interconnect layer 202, a first bonding layer 204, and a second bonding layer 206. The first bonding layer 204 may be disposed between the interconnect layer 202 and a first electrode bulk layer 208 of the SOFC stack, and the second bonding layer 206 may be disposed between the interconnect layer 202 and a second electrode bulk layer 210 of the SOFC stack. That is, the first bonding layer 204 may overlie the interconnect layer 202, and the interconnect layer 202 may overlie the second bonding layer 206. In the embodiment illustrated, the bonding layers 204, 206 are in direct contact with the interconnect layer 202.

[0045] The first electrode bulk layer 208 may be in direct contact with the first bonding layer 204, which may be in direct contact with the interconnect layer 202. The interconnect layer 202 may be in direct contact with the second bonding layer 206, which may be in direct contact with the second electrode bulk layer 210. In the illustrative non-limiting embodiment illustrated in FIG. 2, the first electrode bulk layer 208 includes a cathode bulk layer, and the first bonding layer 204 includes a cathode bonding layer. Further, the second electrode bulk layer 210 includes an anode bulk layer, and the second bonding layer 206 includes an anode bonding layer. That is, in the embodiment illustrated in FIG. 2, the cathode bulk layer overlies the anode bulk layer, with the interconnect layer 202 (and associated bonding layers 204, 206) disposed between the two electrode bulk layers. Alternatively, the anode bulk layer may overlie the cathode bulk layer with the interconnect layer 202 (and associated bonding layers 204, 206) disposed between the two electrode bulk layers. For illustrative purposes only, the first bonding layer 204 and the first electrode bulk layer 208 will be referred to as the cathode bonding layer and cathode bulk layer, respectively. Similarly, the second bonding layer 206 and the second

electrode bulk layer **210** will be referred to as the anode bonding layer and anode bulk layer, respectively.

[0046] In a particular embodiment, the porosity of the cathode bonding layer **204** may be not less than about 5 vol %, such as not less than about 6 vol %, not less than about 7 vol %, not less than about 8 vol %, not less than about 9 vol %, not less than about 10 vol %, not less than about 11 vol %, or even not less than about 12 vol %. Further, the porosity of the cathode bonding layer **204** may be not greater than about 60 vol %, such as not greater than about 55 vol %, not greater than about 50 vol %, not greater than about 45 vol %, not greater than about 43 vol %, not greater than about 41 vol %, or even not greater than about 40 vol %. It will be appreciated that the cathode bonding layer **204** can have a porosity within a range including any of the minimum and maximum values noted above.

[0047] In a particular embodiment, the porosity of the anode bonding layer **206** may be not less than about 5 vol %, such as not less than about 6 vol %, not less than about 7 vol %, not less than about 8 vol %, not less than about 9 vol %, not less than about 10 vol %, not less than about 11 vol %, or even not less than about 12 vol %. Further, the porosity of the anode bonding layer **206** may be not greater than about 60 vol %, such as not greater than about 55 vol %, not greater than about 50 vol %, not greater than about 45 vol %, not greater than about 43 vol %, not greater than about 41 vol %, or even not greater than about 40 vol %. It will be appreciated that the anode bonding layer **206** can have a porosity within a range including any of the minimum and maximum values noted above.

[0048] As an illustrative, non-limiting embodiment, the cathode bonding layer **204** may have an average thickness that is not greater than about 100  $\mu\text{m}$ , such as not greater than about 90  $\mu\text{m}$ , not greater than about 80  $\mu\text{m}$ , not greater than about 70  $\mu\text{m}$ , not greater than about 60  $\mu\text{m}$ , or even not greater than about 50  $\mu\text{m}$ . Further, the cathode bonding layer **204** may have an average thickness that is not less than about 5  $\mu\text{m}$ , not less than about 6  $\mu\text{m}$ , not less than about 7  $\mu\text{m}$ , not less than about 8  $\mu\text{m}$ , not less than about 9  $\mu\text{m}$ , or even not less than about 10  $\mu\text{m}$ . It will be appreciated that the cathode bonding layer **204** can have an average thickness within a range including any of the minimum and maximum values noted above.

[0049] As an illustrative, non-limiting embodiment, the anode bonding layer **206** may have an average thickness that is not greater than about 100  $\mu\text{m}$ , such as not greater than about 90  $\mu\text{m}$ , not greater than about 80  $\mu\text{m}$ , not greater than about 70  $\mu\text{m}$ , not greater than about 60  $\mu\text{m}$ , or even not greater than about 50  $\mu\text{m}$ . Further, the anode bonding layer **206** may have an average thickness that is not less than about 5  $\mu\text{m}$ , not less than about 6  $\mu\text{m}$ , not less than about 7  $\mu\text{m}$ , not less than about 8  $\mu\text{m}$ , not less than about 9  $\mu\text{m}$ , or even not less than about 10  $\mu\text{m}$ . It will be appreciated that the anode bonding layer **206** can have an average thickness within a range including any of the minimum and maximum values noted above.

[0050] The cathode bulk layer **208** may have an average thickness of at least about 0.10 mm, such as least about 0.15 mm, such as at least about 0.20 mm, or even at least about 0.25 mm. Further, the cathode bulk layer **208** may have an average thickness that is not greater than about 2 mm, such as not greater than about 1.9 mm, not greater than about 1.8 mm, not greater than about 1.7 mm, not greater than about 1.6 mm, or even not greater than about 1.5 mm. It will be appreciated that

the cathode bulk layer **208** can have an average thickness within a range including any of the minimum and maximum values noted above.

[0051] The anode bulk layer **210** may have an average thickness of at least about 0.10 mm, such as least about 0.15 mm, such as at least about 0.20 mm, or even at least about 0.25 mm. Further, the anode bulk layer **210** may have an average thickness that is not greater than about 2 mm, such as not greater than about 1.9 mm, not greater than about 1.8 mm, not greater than about 1.7 mm, not greater than about 1.6 mm, or even not greater than about 1.5 mm. It will be appreciated that the anode bulk layer **210** can have an average thickness within a range including any of the minimum and maximum values noted above.

[0052] In a particular embodiment, each of the layers illustrated in FIG. 2 can be formed separately as green layers and assembled together. Alternatively, the layers may be formed in green state in succession on each other. Reference herein to "green" articles is reference to materials that have not undergone sintering to affect densification or grain growth. A green article is an unfinished article that may be dried and have low water content, but is unfired. A green article can have suitable strength to support itself and other green layers formed thereon.

[0053] The interconnect layer **202** may include a lanthanum strontium titanate (LST) material. For example, the interconnect layer **202** may include a doped LST material, such as,  $\text{La}_{0.2} \text{Sr}_{0.8}\text{TiO}_3$ , having one or more dopants. In a particular embodiment, the LST material may be a niobium doped lanthanum strontium titanate (LSTN) material. For example, the LSTN material may have a niobium dopant content that is not less than about 0.01 mol %, not less than about 1 mol %, not less than about 2 mol %, or not less than about 3 mol %. As another example, the LSTN material may have a niobium dopant content that is not greater than about 17 mol %, such as not greater than about 16 mol %, not greater than about 15 mol %, not greater than about 14 mol %, not greater than about 13 mol %, or even not greater than about 12 mol %. It will be appreciated that the niobium dopant content can be within a range including any of the minimum and maximum values noted above. In an illustrative non-limiting embodiment, the niobium dopant content is about 8 mol % (4 mol %  $\text{Nb}_2\text{O}_5$  doped LST, LSTN 4.0).

[0054] The interconnect layer **202** can be a particularly thin, planar layer of material. For example, the interconnect layer **202** may have an average thickness that is not greater than about 100  $\mu\text{m}$ , such as not greater than about 90  $\mu\text{m}$ , not greater than about 80  $\mu\text{m}$ , not greater than about 70  $\mu\text{m}$ , not greater than about 60  $\mu\text{m}$ , or even not greater than about 50  $\mu\text{m}$ . Further, the interconnect layer **202** may have an average thickness that is not less than about 5  $\mu\text{m}$ , not less than about 6  $\mu\text{m}$ , not less than about 7  $\mu\text{m}$ , not less than about 8  $\mu\text{m}$ , not less than about 9  $\mu\text{m}$ , or even not less than about 10  $\mu\text{m}$ . It will be appreciated that the interconnect layer **202** can have an average thickness within a range between any of the minimum and maximum values noted above.

[0055] The interconnect layer **202** can be formed from a powder interconnect material having a particular particle size that facilitates formation of the interconnect cell **200** according to the embodiments herein. For example, the powder interconnect material can have an average particle size of less than about 100 microns, such as less than about 50 microns, less than about 20 microns, less than about 10 microns, less than about 5 microns, or even less than about 1 micron. Still,

in particular instances, the average particle size of the powder interconnect material can be at least about 0.01 microns, at least about 0.05 microns, at least about 0.08 microns, at least about 0.1 microns, at least about 0.2 microns, or even at least about 0.4 microns. It will be appreciated that the powder interconnect material can have an average particle size within a range including any of the minimum and maximum values noted above.

[0056] Materials for the cathode bulk layer 208 generally include lanthanum manganate materials. Particularly, the cathode can be made of a doped lanthanum manganate material, giving the cathode composition a perovskite type crystal structure. Accordingly, the doped lanthanum manganate material has a general composition represented by the formula,  $(La_{1-x}A_x)_yMnO_{3-\delta}$ , where the dopant material is designated by "A" and is substituted within the material for lanthanum (La), on the A-sites of the perovskite crystal structure. The dopant material can be selected from alkaline earth metals, lead, or generally divalent cations having an atomic ratio of between about 0.4 and 0.9 Angstroms. As such, according to one embodiment, the dopant material is selected from the group of elements consisting of Mg, Ba, Sr, Ca, Co, Ga, Pb, and Zr. According to a particular embodiment, the dopant is Sr, and the cathode bulk layer 208 may include a lanthanum strontium manganate material, known generally as LSM. In an exemplary embodiment, the cathode bonding layer 204 may include an LSM material and yttria stabilized zirconia. Coarse particles in the bonding layers may have a puncturing effect. As such, a green LSM powder that is substantially free of coarse particles may be used to form the cathode bonding layer 204. As an illustrative example, substantially all (i.e., 99 vol %) of the LSM particles of the green LSM powder may have a particle size diameter that is less than 10  $\mu m$ .

[0057] Referring to the stoichiometry of the doped lanthanum manganate cathode material, according to one embodiment, parameters such as the type of atoms present, the percentage of vacancies within the crystal structure, and the ratio of atoms, particularly the ratio of La/Mn within the cathode material, are provided to manage the formation of conductivity-limiting compositions at the cathode/electrolyte interface during the operation of the fuel cell. The formation of conductivity-limiting compositions reduces the efficiency of the cell and reduces the lifetime of the SOFC. According to one embodiment, the doped lanthanum manganate cathode material comprises  $(La_{1-x}A_x)_yMnO_{3-\delta}$ , wherein x is not greater than about 0.5, y is not greater than about 1.0, and the ratio of La/Mn is not greater than about 1.0. The value of x within the doped lanthanum manganate composition represents the amount of dopant substituted for La within the structure. In further reference to the stoichiometry of the cathode, the value of y in the general formula  $(La_{1-x}A_x)_yMnO_{3-\delta}$  represents the percent occupancy of atoms on the A-site within the crystal lattice. Thought of another way, the value of y may also be subtracted from 1.0 and represent the percentage of vacancies on the A-site within the crystal lattice. For the purposes of this disclosure, a doped lanthanum manganate material having a value of y less than 1.0 is termed an "A-site deficient" structure, since the A-sites within the crystal structure are not 100% occupied.

[0058] In a particular embodiment, the dopant material is Sr (an LSM cathode), such that the cathode composition is  $(La_{1-x}Sr_x)_yMnO_{3-\delta}$ , where x is not greater than about 0.5, such as not greater than about 0.4, 0.3, 0.2 or even not greater than about 0.1, and particularly within a range of between about

0.3 and 0.05. In a particular embodiment, the value of y is not greater than about 1.0. In an illustrative non-limiting embodiment, x is about 0.2 and y is about 0.98, such that the cathode bulk layer 208 includes an LSM material with a composition of  $(La_{0.8}Sr_{0.2})_{0.98}MnO_3$ . A cathode having an A-site deficient, doped lanthanum manganate composition, as provided in the previously described embodiments, may reduce the formation of conductivity-limiting compositions at the cathode/electrolyte interface during the operation of the fuel cell.

[0059] In a particular embodiment, the anode bulk layer 210 may include a cermet material, that is, a combination of a ceramic and metallic material. For example, the anode bulk layer 210 may be formed with nickel and YSZ. The nickel is generally produced through the reduction of nickel oxide included in the anode precursor, such as a green ceramic composition that is heat-treated. That is, the anode bulk layer 210 may include a nickel oxide and YSZ (before reduction) or nickel and YSZ (after reduction). The anode bonding layer 206 may also include a nickel oxide and YSZ (before reduction) or nickel and YSZ (after reduction). Coarse particles in the bonding layers may have a puncturing effect. As such, a green NiO powder that is substantially free of coarse particles may be used to form the anode bonding layer 206. As an illustrative example, substantially all (i.e., 99 vol %) of the NiO particles of the green NiO powder may have a particle size diameter that is less than 10  $\mu m$ . In a particular embodiment, the YSZ powder that is included in the material that is used to form the anode bonding layer 206 may have a different particle size distribution than the YSZ powder that is included in the material that is used to form the anode bulk layer 210.

## EXAMPLES

[0060] Electrochemical testing was performed for interconnect cells with bonding layers formed from YSZ powders with different PSD types. The particle sizes can be obtained by laser scattering measurements with, for example, a Partica LA-950 laser from Horiba (Horiba Instruments, Inc., Irvine, Calif.).

### Example 1

[0061] An "18-5" YSZ powder (available from Saint-Gobain Corp.) was selected for testing. The 18-5 YSZ powder has a bimodal PSD type with a  $d_{10}$  of 0.71  $\mu m$ , a  $d_{50}$  of 3.66  $\mu m$ , a  $d_{90}$  of 9.31  $\mu m$ , and a specific surface area (SSA) of 1.2  $m^2/g$ .

[0062] A green interconnect cell was sintered to form an integrated, densified interconnect cell. Referring to FIG. 2 for illustrative purposes, the cathode bulk layer 208 included an LSM material with a composition of  $(La_{0.8}Sr_{0.2})_{0.98}MnO_3$  with a thickness of about 1350  $\mu m$ . The anode bulk layer 210 included nickel oxide and YSZ and had a thickness of about 1350  $\mu m$ . The interconnect layer 202 included one "layer" of LSTN 4.0 with a total thickness of about 11  $\mu m$ .

[0063] The cathode bonding layer 204 was formed from the 18-5 YSZ powder and an LSM powder with a composition of  $(La_{0.8}Sr_{0.2})_{0.98}MnO_3$ , having a  $d_{10}$  of 0.58  $\mu m$ , a  $d_{50}$  of 1.38  $\mu m$ , a  $d_{90}$  of 2.69  $\mu m$ , and an SSA of 4.23  $m^2/g$ . The composition of the green cathode bonding layer prior to sintering included 36.70 wt % LSM, 55.05 wt % YSZ, and 8.25 wt % carbon black (c-black as a pore former during sintering). The integrated, densified cathode bonding layer 204 had a thickness of about 25  $\mu m$ .

[0064] The anode bonding layer **206** was formed from the 18-5YSZ powder and a nickel oxide powder with a  $d_{10}$  of 0.46  $\mu\text{m}$ , a  $d_{50}$  of 0.74  $\mu\text{m}$ , a  $d_{90}$  of 1.50  $\mu\text{m}$ , and an SSA of 3.43  $\text{m}^2/\text{g}$ . The composition of the green anode bonding layer prior to sintering included 42.0 wt % NiO and 58.0 wt % YSZ. The integrated, densified anode bonding layer **206** had a thickness of about 25  $\mu\text{m}$ .

[0065] Referring to FIG. 3A, an SEM cross-sectional image **300** illustrates the integrated, densified interconnect cell prior to electrochemical ("E-chem") testing.

[0066] The E-chem testing included heating the interconnect cell to a designed high temperature such as 800° C. and then holding at the high temperature for a designed period with passing fuel (H<sub>2</sub>) in the anode side and oxidant (air) in the cathode side. The NiO in the anode bulk layer and the anode bonding layer is reduced into metallic Ni by the H<sub>2</sub> during heating and holding. A constant current density (such as 0.3 A/cm<sup>2</sup>) was applied into the interconnect cell by two conductive wires (two probes) and two additional conductive wires (two more probes) were used to measure the voltage of the interconnect cell generated by the applied current. This is so called 4-probe method of measuring the resistance. Then the cell resistance and therein the ASR ( $\text{ohms}\cdot\text{cm}^2$ ) can be calculated with the Ohm equation and the interconnect cell active area. The ASR value over time can be dynamically monitored during the long term testing as long as the current is being applied, in order to determine ASR degradation.

[0067] Referring to FIG. 3B, an SEM cross-sectional image **302** illustrates the integrated, densified interconnect cell of FIG. 3A after electrochemical testing. For short term testing, only the initial ASR was measured then the interconnect cell was cooled down to room temperature (usually the test would take only about two days). The image **302** illustrates the puncturing effect from the coarse particles of the 18-5 YSZ powder and associated interconnect cracking.

### Example 2

[0068] A "15-2R2" YSZ powder (available from Saint-Gobain Corp.) was selected for testing. The 15-2R2 YSZ powder has a bimodal PSD type with a  $d_{10}$  of 0.62  $\mu\text{m}$ , a  $d_{50}$  of 2.62  $\mu\text{m}$ , a  $d_{90}$  of 9.56  $\mu\text{m}$ , and a specific surface area (SSA) of 1.93  $\text{m}^2/\text{g}$ .

[0069] A green interconnect cell was sintered to form an integrated, densified interconnect cell. Referring to FIG. 2 for illustrative purposes, the cathode bulk layer **208** included an LSM material with a composition of  $(\text{La}_{0.8}\text{Sr}_{0.2})_{0.98}\text{MnO}_3$  with a thickness of about 1400  $\mu\text{m}$ . The anode bulk layer **210** included nickel oxide and YSZ and had a thickness of about 1400  $\mu\text{m}$ . The interconnect layer **202** included one or two "layers" of LSTN 4.0 with a total thickness of about 27  $\mu\text{m}$ .

[0070] The cathode bonding layer **204** was formed from the 15-2R2 YSZ powder and an LSM powder with a composition of  $(\text{La}_{0.8}\text{Sr}_{0.2})_{0.98}\text{MnO}_3$ , having a  $d_{10}$  of 0.58  $\mu\text{m}$ , a  $d_{50}$  of 1.38  $\mu\text{m}$ , a  $d_{90}$  of 2.69  $\mu\text{m}$ , and an SSA of 4.23  $\text{m}^2/\text{g}$ . The composition of the green cathode bonding layer prior to sintering included 36.70 wt % LSM, 55.05 wt % YSZ, and 8.25 wt % carbon black (c-black as a pore former during sintering). The integrated, densified cathode bonding layer **204** had a thickness of about 25  $\mu\text{m}$ .

[0071] The anode bonding layer **206** was formed from the 15-2R2 YSZ powder and a nickel oxide powder with a  $d_{10}$  of 0.46  $\mu\text{m}$ , a  $d_{50}$  of 0.74  $\mu\text{m}$ , a  $d_{90}$  of 1.50  $\mu\text{m}$ , and an SSA of 3.43  $\text{m}^2/\text{g}$ . The composition of the green anode bonding layer

prior to sintering included 42.0 wt % NiO and 58.0 wt % YSZ. The integrated, densified anode bonding layer **206** had a thickness of about 25  $\mu\text{m}$ .

[0072] The interconnect cell was then subjected to electrochemical testing (as described above in Example 1) over a time period of 1400 hours. Referring to FIG. 4, an SEM cross-sectional image **400** illustrates the integrated, densified interconnect cell after long term testing. FIG. 4 illustrates interconnect cracking, with 43 horizontal cracks identified in the image **400**, and the puncturing effect from the coarse particles.

[0073] FIG. 5 illustrates the results of long term testing of the area specific resistance (ASR) ( $\text{ohms}\cdot\text{cm}^2$ ) of the interconnect cells with bonding layers formed from the 15-2R2 powder. As illustrated in FIG. 5, one interconnect cell with a thin interconnect layer (13  $\mu\text{m}$ ) reached a Steady State ASR within about 500 hours after the start of testing. After reaching the Steady State ASR at about 500 hours, the ASR degraded at a rate of 5.5%/kh; The ASR of another interconnect cell with a thick interconnect layer (27  $\mu\text{m}$ ) was continuously decreased up to 1200 hrs.

### Example 3

[0074] A "17-168" YSZ powder (available from Saint-Gobain Corp.) was selected for testing. The 17-168 YSZ powder has a monomodal PSD type with a  $d_{10}$  of 0.45  $\mu\text{m}$ , a  $d_{50}$  of 0.77  $\mu\text{m}$ , a  $d_{90}$  of 1.5  $\mu\text{m}$ , and a specific surface area (SSA) of 4.32  $\text{m}^2/\text{g}$ .

[0075] A green interconnect cell was sintered to form an integrated, densified interconnect cell. Referring to FIG. 2 for illustrative purposes, the cathode bulk layer **208** included an LSM material with a composition of  $(\text{La}_{0.8}\text{Sr}_{0.2})_{0.98}\text{MnO}_3$  with a thickness of about 1400  $\mu\text{m}$ . The anode bulk layer **210** included nickel oxide and YSZ and had a thickness of about 1400  $\mu\text{m}$ . The interconnect layer **202** included one or two "layers" of LSTN 4.0 with a total thickness of about 13 or 27  $\mu\text{m}$ .

[0076] The cathode bonding layer **204** was formed from the 17-168 YSZ powder and an LSM powder with a composition of  $(\text{La}_{0.8}\text{Sr}_{0.2})_{0.98}\text{MnO}_3$ , having a  $d_{10}$  of 0.58  $\mu\text{m}$ , a  $d_{50}$  of 1.38  $\mu\text{m}$ , a  $d_{90}$  of 2.69  $\mu\text{m}$ , and an SSA of 4.23  $\text{m}^2/\text{g}$ . The composition of the green cathode bonding layer prior to sintering included 36.70 wt % LSM, 55.05 wt % YSZ, and 8.25 wt % carbon black (c-black as a pore former during sintering). The integrated, densified cathode bonding layer **204** had a thickness of about 25  $\mu\text{m}$ .

[0077] The anode bonding layer **206** was formed from the 17-168 YSZ powder and a nickel oxide powder with a  $d_{10}$  of 0.46  $\mu\text{m}$ , a  $d_{50}$  of 0.74  $\mu\text{m}$ , a  $d_{90}$  of 1.50  $\mu\text{m}$ , and an SSA of 3.43  $\text{m}^2/\text{g}$ . The composition of the green anode bonding layer prior to sintering included 42.0 wt % NiO and 58.0 wt % YSZ. The integrated, densified anode bonding layer **206** had a thickness of about 25  $\mu\text{m}$ .

[0078] The interconnect cell was then subjected to electrochemical testing (as described above in Example 1) over a time period of 1000 hours. Referring to FIG. 6, an SEM cross-sectional image **600** illustrates the integrated, densified interconnect cell after long term testing. FIG. 6 illustrates interconnect cracking, with 16 horizontal cracks identified in the image **600**.

[0079] FIG. 7 illustrates the results of long term testing of the area specific resistance (ASR) ( $\text{ohms}\cdot\text{cm}^2$ ) of the interconnect cells with bonding layers formed from the 17-168 powder. As illustrated in FIG. 7, the interconnect cells exhib-

ited rapid ASR degradation substantially immediately after the start of testing. The ASR degraded at a rate of 133%/kh, 308%/kh and 493%/kh, respectively.

#### Example 4

[0080] A “16-191” YSZ powder (available from Saint-Gobain Corp.) was selected for testing. The 16-191 YSZ powder has a monomodal PSD type with a  $d_{10}$  of 0.45  $\mu\text{m}$ , a  $d_{50}$  of 0.84  $\mu\text{m}$ , a  $d_{90}$  of 1.65  $\mu\text{m}$ , and a specific surface area (SSA) of 4.59  $\text{m}^2/\text{g}$ .

[0081] A green interconnect cell was sintered to form an integrated, densified interconnect cell. Referring to FIG. 2 for illustrative purposes, the cathode bulk layer 208 included an LSM material with a composition of  $(\text{La}_{0.8}\text{Sr}_{0.2})_{0.98}\text{MnO}_3$  with a thickness of about 1350  $\mu\text{m}$ . The anode bulk layer 210 included nickel oxide and YSZ and had a thickness of about 1350  $\mu\text{m}$ . The interconnect layer 202 included two “layers” of LSTN 4.0 with a total thickness of about 27  $\mu\text{m}$ .

[0082] The cathode bonding layer 204 was formed from the 16-191 YSZ powder and an LSM powder with a composition of  $(\text{La}_{0.8}\text{Sr}_{0.2})_{0.98}\text{MnO}_3$ , having a  $d_{10}$  of 0.58  $\mu\text{m}$ , a  $d_{50}$  of 1.38  $\mu\text{m}$ , a  $d_{90}$  of 2.69  $\mu\text{m}$ , and an SSA of 4.23  $\text{m}^2/\text{g}$ . The composition of the green cathode bonding layer prior to sintering included 36.70 wt % LSM, 55.05 wt % YSZ, and 8.25 wt % carbon black (c-black as a pore former during sintering). The integrated, densified cathode bonding layer 204 had a thickness of about 25  $\mu\text{m}$ .

[0083] The anode bonding layer 1206 was formed from the 16-191 YSZ powder and a nickel oxide powder with a  $d_{10}$  of 0.46  $\mu\text{m}$ , a  $d_{50}$  of 0.74  $\mu\text{m}$ , a  $d_{90}$  of 1.50  $\mu\text{m}$ , and an SSA of 3.43  $\text{m}^2/\text{g}$ . The composition of the green anode bonding layer prior to sintering included 42.0 wt % NiO and 58.0 wt % YSZ. The integrated, densified anode bonding layer 1206 had a thickness of about 25  $\mu\text{m}$ .

[0084] The SOFC stack including the interconnect cell was then subjected to electrochemical testing (as described above in Example 1) over a time period of 1000 hours. Referring to FIG. 8, an SEM cross-sectional image 800 illustrates the integrated, densified interconnect cell after long term testing. FIG. 8 illustrates interconnect cracking, with 158 horizontal cracks identified in the image 800.

[0085] FIG. 9 illustrates the results of long term testing of the area specific resistance (ASR) ( $\text{ohms}\cdot\text{cm}^2$ ) of the interconnect cell with bonding layers formed from the 16-191 powder. As illustrated in FIG. 9, the interconnect cell reached a Steady State ASR within about 200 hours after the start of testing. After reaching the Steady State ASR at about 200 hours, the ASR degraded at a rate of about 1.9%/kh.

#### Example 5

[0086] A YSZ powder (the “18-48” YSZ powder) was selected for testing, the 18-48 YSZ powder having a monomodal PSD type with a  $d_{10}$  of 0.84  $\mu\text{m}$ , a  $d_{50}$  of 2.14  $\mu\text{m}$ , a  $d_{90}$  of 4.3  $\mu\text{m}$ , and a specific surface area (SSA) of 1.69  $\text{m}^2/\text{g}$ .

[0087] FIG. 10 is an SEM image 1000 of the exemplary 18-48 YSZ powder, and FIG. 11 is a graph that illustrates the particle size distribution of the exemplary 18-48 YSZ powder of FIG. 10. Further details of the particle size distribution of the exemplary 18-48 YSZ powder are included in Table 1.

TABLE 1

Diameter	Frequency %	Oversize %
0.296	0	0
0.339	0.151	0.151
0.389	0.305	0.456
0.445	0.569	1.025
0.51	0.962	1.986
0.584	1.467	3.454
0.669	1.952	5.406
0.766	2.512	7.918
0.877	2.966	10.884
1.005	3.529	14.413
1.151	4.215	18.628
1.318	5.061	23.689
1.51	6.063	29.751
1.729	7.114	36.865
1.981	8.101	44.966
2.269	8.761	53.727
2.599	8.948	62.675
2.976	8.771	71.446
3.409	7.773	79.219
3.905	6.684	85.903
4.472	5.825	91.728
5.122	4.012	95.74
5.867	2.342	98.082
6.72	1.134	99.216
7.697	0.549	99.765
8.816	0.235	100
10.097	0	100

[0088] A green interconnect cell was sintered to form an integrated, densified interconnect cell. FIG. 12 is an SEM cross-sectional image that includes a portion of the integrated, densified interconnect cell. The cathode bulk layer included an LSM material with a composition of  $(\text{La}_{0.8}\text{Sr}_{0.2})_{0.98}\text{MnO}_3$  with a thickness of about 1350  $\mu\text{m}$ . The anode bulk layer included nickel oxide and YSZ and had a thickness of about 1350  $\mu\text{m}$ . The interconnect layer 1202 included two “layers” of LSTN 4.0 with a total thickness of about 36  $\mu\text{m}$ .

[0089] The cathode bonding layer 1204 was formed from the 18-48 YSZ powder and an LSM powder with a composition of  $(\text{La}_{0.8}\text{Sr}_{0.2})_{0.98}\text{MnO}_3$ , having a  $d_{10}$  of 0.58  $\mu\text{m}$ , a  $d_{50}$  of 1.38  $\mu\text{m}$ , a  $d_{90}$  of 2.69  $\mu\text{m}$ , and an SSA of 4.23  $\text{m}^2/\text{g}$ . The composition of the green cathode bonding layer prior to sintering included 36.70 wt % LSM, 55.05 wt % YSZ, and 8.25 wt % carbon black (c-black as a pore former during sintering). The integrated, densified cathode bonding layer 1204 had a thickness of about 25  $\mu\text{m}$ .

[0090] The anode bonding layer 1206 was formed from the 18-48 YSZ powder and a nickel oxide powder with a  $d_{10}$  of 0.46  $\mu\text{m}$ , a  $d_{50}$  of 0.74  $\mu\text{m}$ , a  $d_{90}$  of 1.50  $\mu\text{m}$ , and an SSA of 3.43  $\text{m}^2/\text{g}$ . The cathode bonding layer 1204 had a thickness of about 25  $\mu\text{m}$ . The composition of the green anode bonding layer prior to sintering included 42.0 wt % NiO and 58.0 wt % YSZ. The integrated, densified anode bonding layer 1206 had a thickness of about 25  $\mu\text{m}$ .

[0091] FIG. 12 illustrates that using the 18-48 YSZ powder to form the bonding layers 1204, 1206 results in microstructure and porosity that may improve performance of an SOFC stack.

[0092] The SEM image of FIG. 12 illustrates a microstructure with a substantially uniform thickness of the interconnect layer (IC), the cathode bonding layer (CBL), and the anode bonding layer (ABL). The microstructure further shows good bonding between the IC/ABL and IC/CBL, and a dense IC layer with substantially no defects such as crack free and no puncturing effect caused by the materials in the ABL and CBL. Further, the CBL and ABL have a good porosity, in the

range of between 12 vol % and 40 vol % after reduction (ABL porosity will be increased after NiO is reduced to Ni).

[0093] A particular range of porosity (e.g., about 12 to 40 vol %) after reduction for both ABL and CBL may allow for high performance of an SOFC stack. Porosity in the ABL and CBL that is too high may cause poor bonding and poor contact between the IC/CBL and IC/ABL, resulting in a high ASR for the interconnect cell. Porosity in the ABL that is too low reduces the partial pressure of the fuel (e.g., H<sub>2</sub>) in the interface of IC/ABL and ABL, slowing down or even preventing the NiO reduction in the ABL and the LSTN reduction (LSTN materials have a higher conductivity in reduced condition than in air condition since the reduction of Ti<sup>4+</sup> to Ti<sup>3+</sup> is favored under reduced condition). As a consequence, there is more Ti<sup>3+</sup> when tested under the reduced condition such as in H<sub>2</sub>, which explains the higher conductivities of LSTN materials in fuel gas (H<sub>2</sub>) than in air. Porosity in the CBL that is too low may reduce the partial pressure of the oxygen in the interface of IC/CBL and CBL, reducing the LSM phase stability and increasing the formation of conductivity-limiting compositions at the LSM/YSZ interface during the operation of the fuel cell.

[0094] With respect to porosity, using Image Analyzer software, the porosity of the cathode bonding layer 1204 was estimated to be 16% with a standard deviation of  $\pm 2.0\%$ , and the porosity of the anode bonding layer 1206 was estimated to be 12.6% with a standard deviation of  $\pm 2.1\%$  before NiO reduction.

[0095] FIG. 13 illustrates the pore size distribution of the cathode bonding layer 1204 prior to electrochemical testing. Specifically, FIG. 13 illustrates the frequency of occurrence of pores with a particular maximum length (in microns) in the cathode bonding layer 1204. The mean maximum length of a pore in the cathode bonding layer 1204 is 1.42  $\mu\text{m}$  with a standard deviation of  $\pm 1.28 \mu\text{m}$ .

[0096] FIG. 14 illustrates the pore size distribution of the anode bonding layer 1206 prior to electrochemical testing. Specifically, FIG. 14 illustrates the frequency of occurrence of pores with a particular maximum length (in microns) in the anode bonding layer 1206. The mean maximum length of a pore in the anode bonding layer 1206 is 1.59  $\mu\text{m}$  with a standard deviation of  $\pm 1.55 \mu\text{m}$ .

[0097] An integrated, densified interconnect cell (with bonding layers formed from the exemplary YSZ powder of FIG. 10) was subjected to electrochemical testing (as described above in Example 1) over a time period of 3260 hours. FIG. 15 is an SEM cross-sectional image 1500 showing the interconnect cell after the long term testing. In FIG. 15, the interconnect layer is designated 1502 and the bonding layers are designated 1504 and 1506. After testing for 3260 hours, substantially no cracking was observed in the interconnect layer 1502. Further, there was no puncturing effect associated with coarse YSZ particles (See e.g. FIG. 3B) from either of the bonding layers 1504, 1506.

[0098] FIG. 15 illustrates that, after long term testing, an interconnect cell that includes bonding layers formed from a material that includes a YSZ powder having a monomodal PSD with a d<sub>50</sub> that is greater than 1  $\mu\text{m}$  and a d<sub>90</sub> that is greater than 2  $\mu\text{m}$  (e.g., the "18-48" YSZ powder of Example 5) may exhibit substantially no cracking of the interconnect layer.

[0099] FIG. 16 illustrates the results of long term electrochemical testing (as described above in Example 1) of the area specific resistance (ASR) of two exemplary interconnect cells.

[0100] FIG. 16 illustrates the ASR data associated with an interconnect cell with an interconnect layer that includes LSTN 4.0 with a thickness of about 36  $\mu\text{m}$  (e.g., two "layers" of LSTN 4.0 with a thickness of 18  $\mu\text{m}$  each). An interconnect cell with an interconnect layer having a thickness of about 36  $\mu\text{m}$  corresponds to the interconnect cell 1500 illustrated in the SEM cross-sectional image of FIG. 15 (prior to ASR testing). As shown in FIG. 16, the interconnect cell reached a Steady State ASR within about 1700 hours after the start of testing. That is, the interconnect cell showed no ASR degradation for about the first 1700 hours of testing. Rather, the ASR decreased by about 5%/kh from between 0.18 and 0.20 Ohms· $\text{cm}^2$  at the start of testing to between 0.16 and 0.18 Ohms· $\text{cm}^2$  at about 1700 hours. After reaching the Steady State ASR at about 1700 hours, the ASR degraded at a rate of about 1.9%/kh over the time period from 1700 hours to 3260 hours.

[0101] FIG. 16 further illustrates the ASR data associated with an interconnect cell with an interconnect layer that includes LSTN 4.0 with a thickness of about 18  $\mu\text{m}$  (e.g., one "layer" of LSTN 4.0 with a thickness of 18  $\mu\text{m}$ ). In this case, the interconnect cell reached a Steady State ASR within about 1100 hours after the start of testing. That is, the interconnect cell showed no ASR degradation for about the first 1100 hours of testing. Rather, the ASR decreased at a rate of about 4%/kh from between 0.14 and 0.16 Ohms· $\text{cm}^2$  at the start of testing to between 0.12 and 0.14 Ohms· $\text{cm}^2$  at about 1100 hours. After reaching the Steady State ASR at about 1100 hours, the ASR degraded at a rate of about 3%/kh over the time period from 1100 hours to 3260 hours.

[0102] In the embodiments illustrated in FIG. 16, both the anode bonding layer and the cathode bonding layer were formed from a material that includes the exemplary YSZ powder illustrated in FIG. 10. Thus, using a material that includes a YSZ powder with a monomodal PSD with a d<sub>50</sub> that is greater than 1  $\mu\text{m}$  and a d<sub>90</sub> that is greater than 2  $\mu\text{m}$  (e.g., the YSZ powder illustrated in FIG. 10) in a bonding layer may offer improved ASR performance.

[0103] Referring to FIG. 17, a particular embodiment of a method of forming an integrated SOFC stack is illustrated and generally designated 1700. The method 1700 may include forming a first green cell structure having a first green electrode layer, a green electrolyte layer overlying the first green electrode layer, and a second green electrode layer overlying the green electrolyte layer, at 1702.

[0104] For reference purposes, FIG. 18 illustrates an exemplary SOFC article 1800 that includes multiple green layers to be formed into an integrated SOFC component (e.g., and SOFC stack). As an illustrative example, the method 1700 may include forming a first green cell structure 1802 having a first green electrode layer 1804, a green electrolyte layer 1806 overlying the first green electrode layer 1804, and a second green electrode layer 1808 overlying the green electrolyte layer 1806.

[0105] The method 1700 may include forming a second green cell structure having a first green electrode layer, a green electrolyte layer overlying the first green electrode layer, and a second green electrode layer overlying the green electrolyte layer, at 1704. For example, referring to FIG. 18, the method 1700 may include forming a second green cell

structure **1809** having a first green electrode layer **1810**, a green electrolyte layer **1812** overlying the first green electrode layer **1810**, and a second green electrode layer **1814** overlying the green electrolyte layer **1812**.

**[0106]** The method **1700** may include forming a green interconnect cell disposed between the first green cell structure and the second green cell structure, at **1706**. For example, referring to FIG. 18, the method **1700** may include forming a green interconnect cell **1816** disposed between the first green cell structure **1802** and the second green cell structure **1809**.

**[0107]** In the embodiment illustrated in FIG. 18, the green interconnect cell **1816** includes a green interconnect layer **1818**, a first green bonding layer **1820**, and a second green bonding layer **1822**. As an illustrative, non-limiting embodiment, the green interconnect layer **1818** may include a niobium doped lanthanum strontium titanate (LSTN) material. The first green bonding layer **1820** may be disposed between the green interconnect layer **1818** and the first green cell structure **1802**, and the second green bonding layer **1822** may be disposed between the green interconnect layer **1818** and the second green cell structure **1809**. The first and second green bonding layers **1820, 1822** may include an YSZ powder having a monomodal particle size distribution with a  $d_{50}$  that is greater than 1  $\mu\text{m}$  and a  $d_{90}$  that is greater than 2  $\mu\text{m}$ .

**[0108]** In a particular embodiment, the YSZ powder may have a monomodal medium particle size distribution with a  $d_{90}$  that is greater than 2.5  $\mu\text{m}$ . Further, the YSZ powder may have a monomodal particle size distribution with a  $d_{10}$  that is greater than 0.5  $\mu\text{m}$  or even greater than 0.6  $\mu\text{m}$ . In addition, substantially all particles of the YSZ powder may have a particle size diameter that is less than 10  $\mu\text{m}$ . In a particular embodiment, a specific surface area (SSA) of the YSZ powder may be not greater than 4  $\text{m}^2/\text{g}$ , such as not greater than 3  $\text{m}^2/\text{g}$ , or even not greater than 2.5  $\text{m}^2/\text{g}$ .

**[0109]** The method **1700** may further include sintering (e.g., free sintering, hot pressing) the first green cell structure, the green interconnect cell, and the second green cell structure to integrally bond the first green cell structure, the green interconnect cell and the second green cell structure to form an integrated SOFC stack with densified electrolyte and interconnect layers, at **1708**. For example, referring to FIG. 18, the method **1700** may include sintering the first green cell structure **1802**, the green interconnect cell **1816**, and the second green cell structure **1809** together to integrally bond the first green cell structure **1802**, the green interconnect cell **1816** and the second green cell structure **1809** to form an integrated SOFC cell stack with densified electrolyte and interconnect layers.

**[0110]** In a particular illustrative embodiment, the first green electrode layer **1804** of the first green cell structure **1802** may be a green cathode layer, and the second green electrode layer **1814** of the second green cell structure **1809** may be a green anode layer. In this case, the sintering operation may result in formation of the integrated, densified interconnect cells **200** and **1200** illustrated in FIGS. 2 and 12, respectively.

**[0111]** In a particular embodiment, the YSZ powder that is included in the green anode bonding layer (e.g., the second green bonding layer **1822**) may have a different particle size distribution than the YSZ powder of the green anode layer (e.g., the second green electrode layer **1814**). That is, the YSZ powder that is included in the green anode layer may have a

PSD type other than a monomodal particle size distribution with a  $d_{50}$  that is greater than 1  $\mu\text{m}$  and a  $d_{90}$  that is greater than 2  $\mu\text{m}$ .

**[0112]** The above-disclosed subject matter is to be considered illustrative, and not restrictive, and the appended claims are intended to cover all such modifications, enhancements, and other embodiments, which fall within the true scope of the present invention. Thus, to the maximum extent allowed by law, the scope of the present invention is to be determined by the broadest permissible interpretation of the following claims and their equivalents, and shall not be restricted or limited by the foregoing detailed description.

**[0113]** The Abstract of the Disclosure is provided with the understanding that it will not be used to interpret or limit the scope or meaning of the claims. In addition, in the foregoing Detailed Description, various features may be grouped together or described in a single embodiment for the purpose of streamlining the disclosure. This disclosure is not to be interpreted as reflecting an intention that the claimed embodiments require more features than are expressly recited in each claim. Rather, as the following claims reflect, inventive subject matter may be directed to less than all features of any of the disclosed embodiments. Thus, the following claims are incorporated into the Detailed Description, with each claim standing on its own as defining separately claimed subject matter.

What is claimed is:

1. An interconnect cell of a solid oxide fuel cell stack, the interconnect cell comprising:
  - an interconnect layer;
  - a first bonding layer including yttria stabilized zirconia and having a thickness of not greater than 100  $\mu\text{m}$ ; and
  - a second bonding layer including yttria stabilized zirconia and having a thickness of not greater than 100  $\mu\text{m}$ ,
 wherein the interconnect cell is configured to reach a Steady State Area Specific Resistance within a time period of not less than 600 hours of operation.
2. The interconnect cell of claim 1, wherein the area specific resistance of the interconnect cell is configured to reach the Steady State Area Specific Resistance within a time period of not less than 800 hours.
3. The interconnect cell of claim 1, wherein the area specific resistance of the interconnect cell is configured to reach the Steady State Area Specific Resistance within a time period of not less than 1000 hours.
4. The interconnect cell of claim 1, wherein the first bonding layer has an average thickness of not less than 5  $\mu\text{m}$ .
5. The interconnect cell of claim 1, wherein the second bonding layer has an average thickness of not less than 5  $\mu\text{m}$ .
6. The interconnect cell of claim 1, wherein the area specific resistance of the interconnect cell is not greater than 0.20 ohm  $\text{cm}^2$  after a time period of 3000 hours.
7. The interconnect cell of claim 1, wherein the interconnect layer includes niobium doped lanthanum strontium titanate material.
8. The interconnect cell of claim 1, wherein the interconnect layer has an average thickness of not less than about 5  $\mu\text{m}$  to not greater than about 100  $\mu\text{m}$ .
9. The interconnect cell of claim 1, wherein the first bonding layer is a cathode bonding layer disposed between the interconnect layer and a cathode of the solid oxide fuel cell stack, wherein the cathode bonding layer further includes a lanthanum strontium manganite material.

**10.** The interconnect cell of claim **1**, wherein the second bonding layer is an anode bonding layer disposed between the interconnect layer and an anode of the solid oxide fuel cell stack, wherein the anode bonding layer further includes nickel, nickel oxide, or a combination thereof.

**11.** A solid oxide fuel cell stack, comprising:  
a first electrode layer;  
a first electrolyte layer overlying the first electrode layer;  
a second electrode layer overlying the first electrolyte layer;  
an interconnect cell disposed between the second electrode layer and a third electrode layer of the solid oxide fuel cell stack, the interconnect cell comprising:  
an interconnect layer;  
a first bonding layer disposed between the interconnect layer and the second electrode layer, wherein the first bonding layer includes yttria stabilized zirconia and has an average thickness of no less than 5  $\mu\text{m}$  to not greater than 100  $\mu\text{m}$ ; and  
a second bonding layer disposed between the interconnect layer and the third electrode layer, wherein the second bonding layer includes yttria stabilized zirconia and has an average thickness of no less than 5  $\mu\text{m}$  to not greater than 100  $\mu\text{m}$ ,  
wherein the interconnect cell is configured to reach a Steady State Area Specific Resistance within a time period of not less than about 800 hours of operation;  
a second electrolyte layer overlying the third electrode layer; and  
a fourth electrode layer overlying the second electrolyte layer.

**12.** The solid oxide fuel cell stack of claim **11**, wherein the first bonding layer has a porosity of not less than 5 vol % to not greater than 60 vol %.

**13.** The solid oxide fuel cell stack of claim **11**, wherein the second bonding layer has a porosity of not less than 5 vol % to not greater than 60 vol %.

**14.** The solid oxide fuel cell stack of claim **11**, wherein the interconnect cell is configured to reach a Steady State Area Specific Resistance within a time period of not less than about 1000 hours.

**15.** The solid oxide fuel cell stack of claim **14**, wherein the area specific resistance of the interconnect cell is not greater than about 0.20  $\text{ohm}\cdot\text{cm}^2$  after a time period of about 3000 hours.

**16.** A method comprising operating an interconnect cell such that the interconnect cell reaches a Steady State Area Specific Resistance within a time period of not less than 600 hours, wherein the interconnect cell comprise:

an interconnect layer;  
a first bonding layer including yttria stabilized zirconia and having a thickness of not greater than 100  $\mu\text{m}$ ; and  
a second bonding layer including yttria stabilized zirconia and having a thickness of not greater than 100  $\mu\text{m}$ .

**17.** The method of claim **16**, wherein the time period is not less than 800 hours, and the interconnect cell reaches the Steady State Area Specific Resistance within the time period of 800 hours.

**18.** The method of claim **16**, wherein the time period is not less than 1000 hours, and the interconnect cell reaches a Steady State Area Specific Resistance within the time period of 1000 hours.

**19.** The method of claim **16**, wherein the time period is not less than 1200 hours, and the interconnect cell reaches a Steady State Area Specific Resistance within the time period of 1200 hours.

**20.** The method of claim **16**, wherein the interconnect cell reaches the area specific resistance of not greater than 0.16  $\text{ohm}\cdot\text{cm}^2$  after keeping in heat for a time period of 3000 hours.

\* \* \* \* \*